Energy, Mines and Resources Canada | Énergie, Mines et Ressources Canada

CANMET
Canada Centre for Mineral and Energy Technology | Centre canadien de la technologie des minéraux et de l'énergie

RESULTS OF A LONG-TERM PERSONAL DOSIMETRY PROGRAM AT RIO ALGOM LTD. (QUIRKE MINE)

J. BIGU, B. PALMER AND I. MONTGOMERY

ELLIOT LAKE LABORATORY

NOVEMBER 1986

15 pp

MINING RESEARCH LABORATORIES
DIVISION REPORT MRL 87-49 (TR)

RESULTS OF A LONG-TERM PERSONAL DOSIMETRY PROGRAM AT RIO ALGOM LTD. (QUIRKE MINE)

by

J. Bigu*, B. Palmer** and I. Montgomery***

ABSTRACT

The results of a long-term personal dosimetry program have been analyzed. The program was implemented and carried out at Quirke Mine (Rio Algom Mines Ltd.). The dosimetry program was administered by the Canadian Institute of Radiation Safety (CAIRS). A total of 75 radon/thoron daughter personal dosimeters of the track-etch type were used. The dosimeters employed were the latest prototype developed by the Commissariat de l'Energie Atomique (CEA), France. Dosimeters were worn by workers who volunteered to participate in the program. A total of 48 occupational codes corresponding to 4 major occupational groups were involved. Personal radiation exposure determined by personal dosimetry was compared with exposure estimated from grab-sampling data and personal underground time exposure records.

Broadly speaking, the exposure determined by personal dosimetry was significantly lower than radiation exposures estimated by grab-sampling. Furthermore, poor correlation was found between personal dosimetry and grab-sampling data.

Key words: Radon daughters; Dosimetry; Personal dosimeters

*Research Scientist and Radiation/Respirable Dust/Ventilation Project Leader, Elliot Lake Laboratory, CANMET, Energy, Mines and Resources Canada, Elliot Lake, Ontario.
**Area Ventilation Engineer, ***Ventilation Engineer, Rio Algom Mines Ltd., Elliot Lake, Ontario.

RÉSULTATS DU PROGRAMME A LONG TERME DE DOSIMÉTRIE PERSONNELLE A LA RIO ALGOM LTD. (MINE QUIRKE)

par

J. Bigu *, B. Palmer ** et I. Montgomery ***

RÉSUMÉ

Les résultats du programme à long terme de dosimétrie personnelle ont été analysés. Le programme fut réalisé à la mine Quirke de la compagnie Rio Algom Mines Ltd. Ce programme de dosimétrie a été géré par l'Institut canadien de radioprotection (CAIRS). Au total, 75 dosimètres personnels de type Track-etch, analysant le produit de désintégration du radon et du thoron, ont été utilisés. Ces dosimètres sont les plus récents prototypes développés par le Commissariat de l'Énergie Atomique (CEA) de France. Ces dosimètres ont été portés par des travailleurs qui étaient volontaires pour participer à ce programme. Un total de 48 métiers correspondants à quatre groupes d'occupation majeurs a été impliqué. L'exposition personnelle au rayonnement déterminée à l'aide de ces dosimètres a été comparée à l'exposition telle qu'estimée à partir des données d'échantillonnage au hasard et à partir des registres individuels touchant la durée d'exposition en milieu souterrain.

Globalement nous pouvons affirmer que l'exposition telle que déterminée par les dosimètres personnels a été significativement plus basse que les taux d'exposition obtenus par échantillonnage au hasard. De plus, les corrélations ont été faibles entre les dosimétries personnelles et les données obtenues par échantillonnage au hasard.

MOTS-CLÉS: Produits de désintégration du radon; dosimétrie, dosimètres personnels.

*Chercheur scientifique et Chef de projet en rayonnement, poussières inhalables et ventilation, Laboratoire d' Elliot Lake, CANMET, Énergie, Mines et Ressources Canada, Elliot Lake, Ontario. **Ingénieur en ventilation de surfaces, ***Ingénieur en ventilation, Rio Algom Mines Ltd., Elliot Lake, Ontario.

CONTENTS

TABLES

FIGURES

INTRODUCTION

Personal radiation dosimeters have been developed to estimate the exposure of occupational workers to different kinds of radiation.

A number of personal α-particle dosimeters have been designed to evaluate the exposure to α-particle radiation of underground uranium miners and uranium mill workers. Personal α-particle dosimeters are time-integrating devices that can be of the active kind or the passive type. These dosimeters are usually calibrated in terms of α-particle exposure, e.g., Working Level Month (WLM), or Working Level Hour (WLH).

A personal α-particle dosimeter of the active type consists essentially of a low-power consumption, mechanically reliable, sampling pump, and a sampling head housing a filter facing an α-particle detector. Air flows through the filter where the radon and thoron progeny are deposited. Alpha-particles emitted by the α-particle emitters ^{218}Po, ^{214}Po, ^{212}Bi and ^{212}Po are detected by an appropriate detector, e.g., a thermoluminescent detector (TLD), a track-etch detector (e.g., cellulose nitrate LR-115 and CR-39), or a silicon-diffused, surface-barrier or DRAM (Dynamic Random Access Memory) detector. According to the type of detector used, personal α-particle dosimeters can be classified as TLD dosimeters (TLDD), track-etch dosimeters (TED), or solid-state, electronic, dosimeters (SSED).

Personal α-particle dosimeters of the passive kind do not use a sampling pump and collecting filter, although they can use the same type of α-particle detector and associated electronic circuitry, if required, as active dosimeters.

Thus far, only passive dosimeters, or rather passive monitors, that measure radon gas, ^{222}Rn, concentration have met with design success. This type of device uses a radon-permeable membrane, e.g., polyethelene, that

permits ^{222}Rn to diffuse through into a sensitive volume, where a suitable detector is located, while at the same time removes the radon and thoron progeny. If the diffusivity coefficient of the material is low enough thoron gas, ^{220}Rn, is also removed on account of its short half-life (~55 s).

With the above type of device, ^{222}Rn can be measured fairly accurately. Radon progeny concentration, however, can only be determined if the ratio of radon progeny to radon gas concentration, i.e., the F-coefficient, in air is known. The value for F can vary considerably between 0 and 10 $mWL/pCiL^{-1}$. Usually, an average value of 3 to 5 $mWL/pCiL^{-1}$ is assumed for lack of direct F-data.

Radon progeny passive dosimeters are partly in a state of conceptual development, although several prototypes have been designed and tested. Contrary to the case for active dosimeters, data from radon progeny passive dosimeters have been rather difficult to interpret.

A variety of radon progeny personal dosimeters have been designed and laboratory and field tested in the U.S.A., Canada and other countries (1-9). CANMET has played a very substantial role in instrument development and the laboratory and field evaluation of this instrumentation (10-15).

This report presents data on a radon (thoron) progeny personal dosimetry program at Quirke Mine (Rio Algom Ltd., Elliot Lake, Ontario) during the period 1983 to 1985. This program was requested by the Atomic Energy Control Board and had two major goals in mind:

a) To determine if dosimetry is technically, financially and administratively feasible;

b) To assess the correlation between the present exposure record-keeping method and the dosimetry data.

The data in this report pertains to the use of a track-etch dosimeter (TED) developed by CEA (France), or CEA dosimeter, for short.

ADMINISTRATION OF THE DOSIMETRY PROGRAM

The Canadian Institute for Radiation Safety (CAIRS) at Elliot Lake, (Ont.) was awarded a contract to run the personal dosimetry program. The adminiministration of the program basically consisted of:

a) Ensuring proper operation of the dosimeters by periodically checking the instruments and by applying adequate maintenance procedures;

b) Record-keeping of personnel wearing the dosimeters, and other pertinent data;

c) Retrieving information from the dosimeters;

d) Processing data from the dosimeters, in tabulated form, to Rio Algom Ltd.

Item (a) consisted of:

i) conducting air flow-rate measurements on each dosimeter before and after the exposure period;

ii) cleaning of sampling head in order to remove radioactive contamination;

iii) changing the track-etch film (i.e., detector) after each exposure.

The above operations were performed on a monthly basis.

Item (b) consisted of keeping track of dosimeters (identified by sampling head number and pump number) assigned to personnel (identified by name, occupational code, and other relevant information) participating in the program.

Item (c) consisted of the laboratory processing of the track-etch detector, such as chemical etching and optical counting of the detector tracks rendered visible after the etching process.

Item (d) consisted of the calculation of radiation exposure (WLM) from track counting (see item (c)).

CAIRS was also entrusted with providing the workers with necessary information regarding the aim and goal of the dosimetry program.

The dosimetry program was run on a purely voluntary basis, i.e., only individuals interested in the program would qualify to wear a dosimeter.

In order to obtain a representative picture of the working environment, as many different occupational codes (i.e., occupations) as possible were sought for the program.

The ventilation department at Quirke Mine provided grab-sampling radon progeny data, i.e., Working Level (WL) measurements. Personal exposure by grab-sampling, a standard procedure accepted by AECB, could then be calculated from WL measurements and the time spent by the worker in the different working locations, in the manner described below.

A total of 158 individuals participated in the voluntary dosimetry program for varying lengths of time. They represented four main occupational groups. These groups consisted in turn of occupational sub-groups which were coded according to the specific type of task the individual performed. A total of 48 occupational codes were represented in the main occupational groups. The groups and number of occupational codes within each group are given below. A description of the different occupational codes is given in Appendix A.

Occupational group	Number of Occupational Codes
Mine Department	27
Plant Department	14
Office and Technical	3
"Staff"	4

EXPERIMENTAL PROCEDURE

Each worker participating in the voluntary dosimetry program was assigned a dosimeter which could readily be identified by pump number and sampling head number. When not in use, the dosimeters were plugged into charging racks on surface to ensure full charge for the working shift.

The dosimeters were picked up by the workers shortly before going underground, and were returned to the charging racks at the end of the working shift.

Once each month, the dosimeter heads were taken to CAIRS where the sampling flow rate was measured. The dosimeters were cleaned to remove accumulated contamination, mostly arising from long-lived radioactive dust (LLRD) reaching the collimator and other parts of the sampling head. The track-etch film material from the sampling heads was removed, chemically etched and the tracks developed in the film were counted by means of a semi-automated, computer-based, optical system. Radiation exposure was calculated from track counting as indicated below. The dosimeters were then 'reloaded' with new track-etch material and taken to the charging racks ready for use.

Radon progeny measurements, i.e., Working Level, were conducted at Quirke Mine (Ventilation Dept.) according to the well established and accepted practice of 1 sample/month/working place. This resulted in 20 to 30 samples/day, or 500 to 600 samples/month. Hence, a minimum of about 6000 samples/year were taken. This number of samples represents quite a good sample population for statistical purposes. It should be noted that the above sampling practice of 1 sample/month/location was modified for locations where Working Levels in excess of 0.67 were encountered. In this case, the common sampling practice is 1 sample/week/working place.

Because of manpower and time-constraint considerations, no thoron

progeny measurements were made. The total α-particle count on the grab-sampling filters was used to calculate WL. This total α-count consisted of radon and thoron progeny contributions. The details of this procedure are outlined elsewhere. The method used to calculate WL was the Kusnetz method (16), an accepted method in North America for routine monitoring purposes.

DESCRIPTION OF THE CEA TRACK-ETCH DOSIMETER

The dosimeter consists of a quasi-cylindrically shaped plastic body where a sampling head and a sampling pump of the turbine type are located. The pump is driven by rechargeable batteries that provide electrical power for about 18 h. The batteries are charged in specially designed racks by magnetic induction.

The sampling head includes a filter holder with a 0.8 μm Millipore filter facing a track-etch detector film. The filter and track-etch detector are separated by three collimators which expose three different areas of the track-etch film to the filter. The exposed areas of the track-etch material are covered with three different thicknesses of an α-absorbed, i.e., polycarbonate material, to detect α-particles of different energy from radon and thoron progeny sampled in the filter.

Detection of α-particles is done by cellulose nitrate film (Kodak Pathé LR115), the track-etch detector. The sensitive layer of the film is 13 μm thick and red, and is mounted in a colourless Mylar film.

The passage of α-particles through the cellulose nitrate affects the structure of the substance in such a way that if the energy of the incident particle is properly chosen, and appropriate chemical etching is applied, holes of regular dimensions in the detector with diameters of several μm are produced. Detection of radon and thoron progeny α-emitters are effected by polycarbonate absorbers of different thicknesses placed on the detectors as

follows.

The distance covered by the α-particles in the air and the thickness of the absorber is such that at the end of a collimator the α-particles emitted by ^{218}Po (RaA) and ^{214}Po (RaC') do not emerge from the absorber, whereas those emitted by ^{212}Po (ThC') emerge with a residual energy of about 3 MeV and are thus recorded. At the end of the second collimator the α-particles emitted by ^{214}Po emerge with a residual energy of 3 MeV and are recorded, whereas α-particles from ^{218}Po (above 5 MeV) do not leave any tracks with present etching conditions. At the end of the third collimator, α-particles emitted by ^{214}Po and ^{212}Po have energies greater than 5.3 MeV and do not give tracks in the detector film, whereas α-particles from ^{218}Po emerge with an energy of 2.8 MeV and are recorded.

Tracks produced in the detector appear as luminous white patches on a red background. Tracks can be counted using an optical microscope, a spark detector, or by evaluating the density of tracks through the quantity of light transmitted by these holes.

The number of tracks on each area of the track-etch film is related to the respective radionuclide decay rate, and hence to its airborne activity concentration. Track counting, therefore, allows evaluation of the radon and thoron progeny concentrations, and of the Working Levels. As indicated below, track counting also permits the calculation of radiation exposure.

CALCULATION OF RADIATION LEVELS AND RADIATION EXPOSURE

In this report the term radiation level is loosely employed to indicate radon and thoron activity concentrations, or Working Levels. More specifically, however, progeny activity concentrations (pCi/L or mBq/m^3) are indicated by square brackets, i.e., $[^{218}Po]$, whereas Working Levels are indicated either by WL(Rn), radon progeny Working Level, or WL(Tn), thoron

progeny Working Level. When no specific reference to WL(Rn) or WL(Tn) is meant, the Working Level is simply referred to as WL. For other special cases, other terminologies are used.

Radiation exposure is measured in Working Level Hours (WLH), or more preferably, in Working Level Month (WLM). The relationship between WLM and WLH is a simple one, namely:

$$WLM = WLH/170 \qquad \text{Eq 1}$$

where,

$$WLH = WL \times T_{exp} \qquad \text{Eq 2}$$

T_{exp} is the exposure time and is given in hours (h). The numerical coefficient 170 represents the average number of working hours in a month.

A. TRACK-ETCH DOSIMETER

Radiation exposure is calculated from experimental data by the dosimeter as follows:

$$WLM(Rn) = \frac{7.7\ N(RaC') + 5.99\ [N(RaA) - 1/2\ N(ThC')]}{1.06 \times 10^{-3} \times 170 \times 1.3 \times 10^{5} \times Q}$$

$$= 0.4269 \times 10^{-4} \left\{ \frac{7.7\ N(RaC') + 5.99\ [N(RaA) - 0.5\ N(ThC')]}{Q} \right\} \qquad \text{Eq 3}$$

where, N(RaA), N(RaC') and N(ThC') are the number of tracks measured in the detector above the appropriate absorber. The numerical coefficient 1.06×10^{-3} is the overall efficiency of the system. The number 1.3×10^{5} represents (in MeV) the total potential α-particle energy from the short-lived progeny in a litre (L) of air at WL = 1. The symbol Q is the sampling flow rate of the dosimeter given in Lh^{-1}. The symbol Rn in WLM is used to indicate radon progeny, hence WLM(Rn) indicates radon progeny exposure in Working Level Month.

Similarly, for the thoron progeny, WLM(Tn) is given:

$$WLM(Tn) = 0.4269 \times 10^{-4} \left(\frac{11.74\ N(ThC')}{Q} \right) = 5.012 \times 10^{-4}\ [N(ThC')/Q] \qquad \text{Eq 4}$$

It should be noted that for precise calculation of WLM(Rn) and WLM(Tn),

the contribution from long-lived radionuclides should be taken into consideration. This contribution arises from contamination in the sampling heads by long-lived radioactive dust (LLRD), as shown in reference 15. The contribution to the number of tracks from LLRD contamination poses a limit to the accuracy with which WLM(Rn) and WLM(Tn) can be determined.

B. GRAB-SAMPLING MEASUREMENTS AT QUIRKE

Routine Working Level measurements carried out by the Ventilation Dept. at Quirke were used as part of the dosimetry program to compare the two approaches for calculating personal radiation exposure, namely: by personal dosimetry using the track-etch dosimeter, and by grab-sampling area monitoring following Rio Algom's accepted practice using Equations 1 and 2, i.e.,

$$WLM = \left(\frac{1}{170}\right) \Sigma_i (WL)_i \; T_{exp,i} \qquad \text{Eq 5}$$

where, the subindex i is used to indicate location, and the sigma sign is used to denote summation over all locations i. Equation 5 simply indicates that the radiation exposure for a given individual can be evaluated if Working Level measurements at the different locations where the worker spends time, i.e., $(WL)_i$, and the times spent at the different working locations, i.e., $T_{exp,i}$, are known. These data are collected by Rio Algom on a periodic basis.

Working Level measurements were carried out using the Kusnetz method (16).

$$WL(Rn) = \frac{N_\alpha}{QT_s \epsilon K} \qquad \text{Eq 6}$$

where, Q is the sampling flow-rate (L/min);

T_s is the sampling time (min);

ϵ is the α-counting efficiency of the scaler used;

K is the so-called Kusnetz factor which depends on the time at which the count is done; and

N_α is the net α-particle count rate in counts per minute (cpm).

The following values for the above variables were used at Quirke: Q = 5-6 L/min, T_s = 3 min, ϵ ~0.4, and K = 100 corresponding to a waiting time of ~65 min. The α-particle counting time was 1 min.

As an error analysis can readily show, short sampling times, and even shorter counting times at low radiation levels can result in significantly reduced accuracy in the determination of WL(Rn).

It should be noted that because no thoron progeny measurements were done, N_α in Equation 6 represents in fact the total α-count rate, i.e., radon and thoron progeny combined. Hence, WL(Rn), as calculated above has been systematically overestimated by an amount which depends on the ratio WL(Tn)/WL(Rn). Grossly speaking, WL(Tn)/WL(Rn) ~0.5 to 0.8, results in WL(Rn) being overestimated, on average, by 10-15%.

MEASUREMENT OF DOSIMETER (PUMP) FLOW RATE

The sampling periods lasted for a full month at a time. The pump flow rate for each dosimeter was measured twice per month:

i) when a fresh filter was installed in the sampling head before the beginning of the sampling period, i.e., first of the month; and

ii) at the end of the sampling period, i.e., end of the month.

The dosimeters were in operation for 29 months (February 1983 to June 1985). During this period the method of flow rate measurement and calculation of flow rate changed on a number of occasions. In all cases, because of the mechanical design and geometry of the dosimeters, flow rate measurements could not be done at the sampling head intake. Measurements were conducted at the exhaust using the dosimeter in its usual field configuration, or only part thereof as follows:

a) From February 1983 to July 1983, measurements were carried out with a mass

flowmeter using the dosimeter in its usual field configuration.

b) From August 1983 to March 1984, no direct flow rate measurements were done. Flow rates were calculated from pressure measurements using a magnehelic gauge and the following empirical expression:

$$Q = 8.45\ \overline{TP} \qquad \text{Eq 7}$$

where $\overline{TP}$ = (TP1 + TP2)/2. The symbols TP1 and TP2 stand for turbine (pump) pressure at the beginning and end of the month, respectively. The turbine pressure was measured by means of the magnehelic gauge. The numerical factor 8.45 represents the slope of a linear regression fit through data points representing TP against Q, the latter measured by a mass flowmeter. It should be noted that if the flow rate of the dosimeter calculated with Equation 7 was less than 3 Lh^{-1}, the flow rate was assumed to be 3 Lh^{-1} anyway. This was done because it was assumed that the decrease in Q after continuous operation was caused by excessive dust filter loading at an indeterminate time during the month; and

c) From April 1984 to June 1985, no direct flow rate measurements were conducted. Flow rates were calculated using Equation 8 following the two-step experimental procedure indicated below:

i) The dosimeter head was removed from the dosimeter body, and a specially designed hollow coupling device was fitted, leak free, to the turbine pump of the dosimeter. The coupling device was provided with a special fitting that could be connected via plastic tubing to a magnehelic gause, which measured, as before, the turbine pump pressure, TP, when the pump was in operation.

ii) The sampling head in its usual field, i.e., sampling, configuration was fitted to a Gilian pump, set at the same flow rate as the dosimeter pump, and to a magnehelic gauge connected in parallel. This

arrangement allowed the filter resistance, FR, before and after the sampling period, i.e., FR_1 and FR_2, respectively to be measured. The pump flow rate was then calculated according to:

$$Q = 2[(TP_1/FR_1) + (TP_2/FR_2)] \qquad \text{Eq 8}$$

where, TP_1 and TP_2 have their usual meaning (see item b).

In order to determine more precisely the flow rate characteristics of the dosimeters under field conditions, a series of very careful flow rate measurements were also conducted by CAIRS at the request of Rio Algom Ltd. for a period of two weeks. During this period two flow rate measurements per day for each dosimeter were made: one before the start of the work shift, and one at the end of the work shift.

LONG-LIVED RADIOACTIVE DUST AND CONTAMINATION MEASUREMENTS

Strong contamination of the dosimeters sampling heads has been observed in early CEA prototypes (15), and in more recent ones. The source of contamination has been traced to accumulation of long-lived radionuclides associated with dust in the respirable range in the collimators, and perhaps other parts of the sampling head. Because of the contamination problem, and because of its interest in health-related issues, Long-Lived Radioactive Dust (LLRD) collected on the filter was examined, and measured, every time the filters were changed at the end of the month. A measure of the LLRD concentration in air (mBq/m^3), and its specific activity in the filter (mBq/mg dust) would provide an indication of the potential contamination to be expected. It would also give some idea of the LLRD concentration in the three energy channels of the dosimeter, i.e., some α-particles from the LLRD are expected to reach the absorbers on the track-etch film with the energy required to produce tracks.

EXPERIMENTAL RESULTS AND DISCUSSION

The dosimetry program extended over a period of about 2 1/2 years. A great deal of data were collected during this time. However, only representative and selected data are presented in this report. The results have been summarized in Tables 1 to 6, and Figures 1 to 30.

The symbols $(WLM)_{T,GS}$ and $(WLM)_{DOS}$ used in the above Figures have the following meaning:

a) $(WLM)_{T,GS}$ stands for total Working Level Month calculated from grab-sampling data (see Equations 5 and 6). It should be noted that only WL(Rn) has been used here as WL(Tn) was not experimentally measured. As previously indicated, WL(Rn) has been systematically overestimated because N_α in Equation 6 includes the α-particle thoron progeny contribution.

b) $(WLM)_{DOS}$ stands for total Working Level Month calculated from dosimetry data (see Equations 3 and 4). The total WLM for the dosimeters was calculated according to the standard procedure indicated by Equation 9:

$$(WLM)_{DOS} = WLM(Rn) + 1/3\ WLM(Tn) \qquad \text{Eq 9}$$

The horizontal bar in some graphs is used to indicate average values.

For the sake of simplicity, the results and discussion section have been divided into three main subsections, namely: dosimeters sampling flow rate data; dosimetry and grab-sampling data; and Long-Lived Radioactive Dust (LLRD) data, and other data.

A. DOSIMETERS SAMPLING FLOW RATE DATA

Some flow rate data for the dosimeters have been summarized in Tables 1 and 2, and Figures 1 to 7.

Figures 1 to 3 show typical flow rate data for three dosimeters. The data extend over the period over which the dosimeters were fully operative, i.e., 1983/1985, see also Table 1. Each bar in the graphs represents the

average of two flow-rate measurements per month.

Figure 4 shows the calculated monthly averaged flow rate corresponding to all the dosimeters used in the personal dosimetry program at Quirke Mine. A total of 75 dosimeters were used.

The data reproduced in Figures 1 to 4 have been calculated from flow rate measurements carried out by CAIRS.

CAIRS staff undertook the task of verifying flow rate data by measuring the flow rate of all the dosimeters for a period of two weeks using a special flow rate meter (see below). Each dosimeter was measured twice daily, before the work shift, and after the dosimeters were brought back to surface. Some of the data obtained are given in Table 2, and Figures 5 and 6. Flow rate data for six dosimeters have been plotted in Figures 5 and 6.

The 'overall' monthly average flow rate obtained for all dosimeters combined given in Figure 4 shows a somewhat irregular steady decrease in value from February 1983 to March 1984 at which time the flow rate increased substantially and maintained an almost constant value until the end of the dosimetry program. This experimental observation seems to suggest a systematic bias in the air flow rate measurements which roughly coincides with the time at which different flow rate measurement methods and techniques were applied. The mean air flow rate over the entire program (February 1983 to June 1985) was 3.99 ± 0.37 Lh^{-1}, the standard deviation, σ, from the mean being about 10% of the mean. In addition, the ratio of maximum flow rate, Q_{max}, to minimum flow rate, Q_{min}, observed was: $Q_{max}/Q_{min} = 1.33$, which corresponds to a variation of about 33% (see Table 1).

However, flow rate data for the three dosimeters chosen for illustration purposes (see Figures 1 to 3) clearly show a less well defined behaviour than the data of Figure 4. This is understandable as data are now being treated on an individual basis, and hence the dosimeter flow rate

variations are more evident. Data from the above Figures and Table 1 for dosimeters 42, 94 and 29 give the following values 4.04 $\pm$ 0.41 Lh^{-1}, 3.88 $\pm$ 0.68 Lh^{-1}, and 3.88 $\pm$ 0.71 Lh^{-1}, respectively. Hence the values for $(\sigma/\overline{Q})$ x 10^2, are respectively: 10.1%, 17.5% and 18.3%, i.e in the range 10 to 20%. The ratio Q_{max}/Q_{min} was, however, quite variable. In the case of these three dosimeters the ratio was 1.38, 1.74 and 1.92 for dosimeters 42, 94 and 29, respectively. These values suggest that strong month to month flow rate variations were the rule and not the exception. The above values for the ratio Q_{max}/Q_{min} represent variations of 38% to 92%.

Because of the above, large variations in the exposure levels measured by the dosimeters under the same environmental, i.e., radiation, conditions are to be expected on account of the observed air flow rate differences alone. It should be noted that the variations in the flow rate observed cannot be attributed to dust filter loading only as measurements using a clean filter and a moderately dust loaded filter were not significantly different.

The data in Table 2 and Figures 5 and 6 show that air flow rate variations were in general smaller than those indicated by Figures 1 to 3. This is to be expected as in this case more time, effort and care, and perhaps more accurate instrumentation, was employed. The ratio $\sigma/\overline{Q}$ for these measurements was less than 20%. In spite of this time consuming exercise, the accuracy of the flow rate measurements was not markedly improved. It should be noted that in this case an automated bubble test flow calibrator, known under the commercial name Buck Calibrator, manufactured by Gilian (U.S.A.), was used.

An observation is worth mentioning, namely the flow rate of the CEA track-etch dosimeter should not be measured before 1 hour of continuous operation. This is so because of the characteristics of the turbine pump used which exhibits a high flow rate at the beginning followed by a steady decrease

to a constant value after a 'warm-up' period of about 1 h. This behaviour is shown in Figure 7 for a given dosimeter, and is typical of all CEA dosimeters. The ratio Q_{max}, i.e., flow rate at time 0, to the steady-state flow rate, Q_{ss}, is $Q_{max}/Q_{ss} = 1.19$.

The fact that the dosimeter flow rate is higher than normal for a period of about an hour indicates that a systematic overestimation of the Working Level will be in effect. However, since most of this time is spent by the worker in areas of low radiation exposure, e.g., waiting for the cage and travelling down in the cage to the work place, this higher than normal flow rate is not expected to contribute significantly to the total daily radiation exposure measured by the dosimeter.

The above discussion can be summarized as follows:

1. Analyses of flow rate data do not show significant differences when 'overall' (i.e., over 2 1/2 year period) flow rate averages for all dosimeters combined, on a monthly basis, are compared with the 2-week period indicated above, i.e., $\overline{Q} = 3.99 \pm 0.37$ Lh^{-1} versus $\overline{Q} = 3.77 \pm 0.38$ Lh^{-1}, respectively. In both cases, $\sigma \sim 0.1\ \overline{Q}$ Lh^{-1}, i.e., about 10%. The difference between $\overline{Q}$ being about 6%.
2. Quite significant month to month variations in the measured flow rate for each dosimeter were noted. Hence, large fluctuations in the reported radiation exposure level (WLM) by the dosimeters are expected on account of these flow-rate variations alone. This problem arises from limiting the number of flow rate measurements per dosimeter to two per month.
3. Based on individual flow rate data, radiation exposure by the dosimeter cannot be expected to be accurate to better than about 30 to 50% on a single measurement.

B. DOSIMETRY AND GRAB-SAMPLING DATA

Part of the dosimeters and grab-sampling data collected are presented in Figures 8 to 29, and Tables 3 to 6.

Figures 8 to 14 show radiation exposure as calculated from dosimetry data, $(WLM)_{DOS}$, and grab-sampling data, $(WLM)_{T,GS}$ versus time for several occupational codes. Also shown in the graphs are the calculated average values for $(WLM)_{DOS}$ and $(WLM)_{T,GS}$ during the dosimetry program. These Figures represent typical examples. The main conclusions that can be drawn from an analysis of these data are the following:

1. In a number of cases there was a fair to good temporal correlation between $(WLM)_{DOS}$ and $(WLM)_{T,GS}$, as shown by Figures 8 to 10. However, more often than not, poor temporal correlation between these two variables was observed (see Figures 11 to 14).
2. On rare occasions both good temporal and good quantitative agreement was simultaneously attained for $(WLM)_{DOS}$ and $(WLM)_{T,GS}$.
3. Although poor quantitative agreement between $(WLM)_{T,GS}$ and $(WLM)_{DOS}$ was observed on a monthly basis, the average values for these two variables taken over the entire dosimetry program were found to agree within 10%, i.e., better than experimental error (see Figures 10 and 12).
4. In many instances poor to very poor temporal and quantitative correlation was found between $(WLM)_{DOS}$ and $(WLM)_{T,GS}$, as shown by Figures 13 and 14.
5. Strong month to month fluctuations in dosimetry and grab-sampling radiation exposure levels were observed. From the data it could not be ascertained whether $(WLM)_{DOS}$ behaved better, statistically speaking, than $(WLM)_{T,GS}$, or vice versa. Hence, specific and/or systematic biases (errors) could not be easily established.
6. There was no specific extended period of time, e.g., year, during which items 1 to 5 showed any significant improvement over any other period.

Item 3 is particularly disturbing because it indicates that it is possible, and frequent, to have large monthly discrepancies between $(WLM)_{DOS}$ and $(WLM)_{T,GS}$ while still having close agreement between the radiation exposures by these two methods calculated over extended periods of time.

Figures 15 to 17 show frequency histograms of $(WLM)_{DOS}$ and $(WLM)_{T,GS}$. The graphs show the number of times dosimetry and grab-sampling readings were within a given WLM range. The Figures show that over 80% of the values obtained for $(WLM)_{T,GS}$ and $(WLM)_{DOS}$ were below 0.2 WLM (see Table 3). However, the frequency distributions were different for these two variables, namely the maximum corresponding to the $(WLM)_{T,GS}$ histograms were higher than those corresponding to $(WLM)_{DOS}$. In other words, either $(WLM)_{DOS}$ was underestimated or $(WLM)_{T,GS}$ was overestimated, or both.

The data presented in Figures 15 to 17 represent an excellent statistical sample population, namely 1728 independent $(WLM)_{DOS}$ measurements and the same number of independent measurements of $(WLM)_{T,GS}$, i.e., a total of 3456 measurements.

Figures 18 to 23 show $(WLM)_{T,GS}$ versus $(WLM)_{DOS}$ for 1983, 1984 and 1985 for several occupations: driller, slusherman, diamond driller, timberman, level serviceman (track), and mine shift boss.

Best fitted lines by linear regression analysis were drawn through experimental data points. Each Figure contains three independent graphs which represent the best fitted straight line for each year of the dosimetry program, i.e., 1983, 1984 and 1985.

The results of Figures 18 to 23 represent typical data selected for the purpose of illustration. Statistical and analytical data pertaining to these Figures have been tabulated in Table 4. Similar data for all the other occupations or occupational codes have been summarized in Table 5.

Figures 18 to 23 and Tables 4 and 5 show that in most cases only fair

to poor correlation between $(WLM)_{T,GS}$ and $(WLM)_{DOS}$ was attained. Good correlation between these two variables was found in only a few cases. Furthermore, data for a mine shift boss (see Figure 23) were not any better than for any other worker indicating that higher position, and hence more responsibility, and presumably more care regarding the use of the dosimeter, was not a guarantee of a better result. Table A.2 (Appendix) shows data similar to that of Table 5, but for all occupations on a yearly basis.

An analysis of all data thus far obtained does not conclusively indicate that the poor correlation found between $(WLM)_{DOS}$ and $(WLM)_{T,GS}$ can specifically be attributed to a given year, period (i.e., season) within a year, or any given occupational code(s).

Figures 24 to 26 show data similar to those presented in Figures 18 to 23, but for all dosimeters, i.e., occupational codes, within each year of the dosimetry program. The parameters pertaining to the best fitted straight lines through the experimental data points are given in Table 6. The data of Figures 24 to 26 and Table 6 again show a rather poor correlation between $(WLM)_{DOS}$ and $(WLM)_{T,GS}$. This result only confirms what has already been shown and discussed above.

Figure 27 shows $(WLM)_{Tn,DOS}$ versus $(WLM)_{Rn,DOS}$, where Tn and Rn stand for thoron progeny and radon progeny, respectively. These data are dosimetry data and because each data point on the graph represents a pair of values regarding the same dosimeter(s), the graph is equivalent to WL(Tn) versus WL(Rn). It should be noted that each data point in Figure 27 represents the average of $(WLM)_{Tn,DOS}$ and $(WLM)_{Rn,DOS}$ for each individual for all time during which data were available. A total of 157 values were calculated for the 1983/85 period and plotted in Figure 27. Best fitter curves by regression analysis have been drawn through the data points. Two analytical curves were fitted through the data, namely a power curve and a straight line. The

expressions obtained by the regression analyses are as follows:

$$(WLM)_{Tn,DOS} = 0.5684(WLM)_{Rn,DOS}^{1.006}, \text{ and} \qquad \text{Eq 10}$$

$$(WLM)_{Tn,DOS} = 0.4746(WLM)_{Rn,DOS} + 0.0079 \qquad \text{Eq 11}$$

Figure 27 indicates a better fit for low and intermediate values of $(WLM)_{Tn,DOS}$ and $(WLM)_{Rn,DOS}$ for the power equation than for the linear relationship. The correlation coefficient for Equation 11 was approximately 0.89. No similar data by grab-sampling are available as WL(Tn) was not measured. The above relationships are important because if consistently constant they can be used to calculate $(WLM)_{Tn}$ or WL(Tn) from field determinations of $(WLM)_{Rn}$ by dosimetry or WL(Rn) by grab-sampling. Equations 10 and 11 are not expected to remain constant if air flow conditions vary drastically. However, they are expected to remain roughly constant over large sections of the mine providing air flow changes are moderate. The above relationships are also dependent on the characteristics of the rock formation and the gram mass ratio $^{238}U/^{232}Th$ (17).

Figures 28 and 29 show, respectively $(WLM)_{DOS}$ and $(WLM)_{T,GS}$ versus time, i.e., month within a given year, and year. Each value represents the average of all dosimeter readings during a given month and year (Figure 28), or the average of all grab-sampling measurements taken during a given month and year (Figure 29).

Some relevant data from Figures 28 and 29 are given below:

$$(WLM)_{DOS,min} = 0.0398 \text{ (July 1984)}$$

$$(WLM)_{DOS,max} = 0.1301 \text{ (March 1985)}$$

$$(WLM)_{DOS} \pm \sigma = 0.085 \pm 0.026 \text{ (January 1983 - June 1985)}$$

$$(WLM)_{DOS,max}/(WLM)_{DOS,min} = 3.27$$

$$(\sigma/(WLM)_{DOS}) \times 10^2 = 30.5\%$$

where, the indices min and max are used to indicate minimum and maximum,

respectively. Furthermore:

$$(WLM)_{T,GS,min} = 0.094 \text{ (December 1984)}$$

$$(WLM)_{T,GS,max} = 0.171 \text{ (February 1983)}$$

$$(\overline{WLM})_{T,GS} \pm \sigma = 0.134 \pm 0.019 \text{ (January 1983 - June 1985)}$$

$$(WLM)_{T,GS,max}/(WLM)_{T,GS,min} = 1.82$$

$$(\sigma/(\overline{WLM})_{DOS}) \times 10^2 = 14.2\%.$$

The above data and Figures 28 and 29 show the following rather striking experimental findings:

1. The monthly variations in WLM for all dosimeters combined were significantly larger than the monthly WLM monthly variations for the combined grab-sampling measurements.
2. Item one is clearly reflected in the maximum to minimum WLM ratios for the dosimeters and by grab-sampling which were, respectively 3.27 and 1.82, i.e., a twofold factor, approximately.
3. The mean WLM for all dosimeters combined over the entire dosimetry program was significantly lower than the WLM for all grab-sampling data combined over the same period of time, i.e., $(\overline{WLM})_{DOS}/(\overline{WLM})_{T,GS} = 0.63$. This suggests a systematic underestimation of radiation exposure by the dosimeters, or conversely a systematic overestimation of exposure by grab-sampling data, or both.
4. Further evidence for the unexpectedly strong monthly variations of dosimetry data is given by the ratio $\sigma/\overline{WLM}$ which was ~30% for the dosimeters as opposed to approximately 14% for grab-sampling data.

One would expect dosimetry data to show far less monthly variations than grab-sampling data. This is so because dosimetry data represent data averaged by the dosimeter over a 170 h/month period, whereas grab-sampling data represent measurements taken with a sampling time of 3 min, and an α-particle count of 1 min. Hence, statistically speaking grab-sampling

measurements are conducted under somewhat unfavourable conditions and the errors associated with grab-sampling are expected to be relatively high. This, however, is partly offset by the larger number of grab-sampling measurements compared with dosimetry measurements. The significant dosimeters data deviation from the mean value seem to be related to fluctuations in the measured monthly dosimeter flow rate, and also to the contribution to the total number of tracks from LLRD collected in the filter, and LLRD contamination in the sampling head.

C. LONG-LIVED RADIOACTIVE DUST DATA AND OTHER DATA

Long-Lived Radioactive Dust (LLRD) deposited on the filters was measured on a regular basis as previously indicated. Figure 30 shows a normalized frequency distribution histogram for LLRD. The graph shows a wide range of values for the airborne LLRD concentration, and therefore, the LLRD activity in the filter. Most measurements were in the range 10-150 mBq/m^3. The graph shows a multivalued LLRD concentration function with maxima at about 40, 70, and 120 mBq/m^3. An approximate average value of 50 mBq/m^3 can be assumed for practical purposes and rough calculations. A more exact value can be derived from Figure 30.

With the above data some indication of the contribution of LLRD to dosimeter track readings can be obtained. The number of α-particles reaching each absorber, with the right energy to produce a nuclear track during the monthly exposure period, i.e., N'_α, can be calculated using the following expression:

$$N'_\alpha \sim 60 \times 10^{-3} \times 170 \times 60\, A(QT_s)(S/S_T)(1/3)\delta\eta C_F$$

$$= 2.04 \times 10^2\, A(QT_s)(S/S_T)\delta\eta C_F \qquad \text{Eq 12}$$

where, in the above equation:

A is the airborne LLRD activity concentration (mBq/m^3);

Q is the dosimeters sampling flow rate (~4 Lh^{-1});

T_s is the month exposure time ($\bar{<}$170 h in most cases);

S_T is the total surface area of the track-etch film;

S is the total cross-sectional area corresponding to the three collimators used in the dosimeters sampling head. Hence, the ratio $(S/S_T)(1/3)$ respresents the cross-sectinal area of one collimator;

δ is the probability of an α-particle emitted from the filter to reach the absorber with the right energy to produce a nuclear track in the film;

η is a correction factor applicable to δ as follows: If the α-particle is emitted by the filter, η=1. However, if LLRD reaches other parts of the dosimeters sampling head, e.g., collimator walls, η is most likely to be greater than unity; and

C_F is a correction factor, to be applied to A, to take into account LLRD deposited in parts of the sampling head other than the dosimeter filter. For LLRD deposited in the filter C_F=1. For LLRD deposited in other parts of the sampling head, i.e., contamination of the collimator walls, $C_F \neq 1$.

Because the energy of α-particles emitted by long-lived radionuclides are lower than those from the radon and thoron progenies, the contribution from LLRD deposited in the filter, calculated with Equation 12, is expected to be very small. This is so because of the physical dimensions and geometry of the sampling head. However, the contribution from LLRD deposited, in say collimator walls, can be quite significant. Deposition in the collimator walls and other parts of the sampling head, except the filter, can only be explained if the system is not air tight allowing air leaks to reach the collimators and other parts of the dosimeter.

An approximate calculation of N'_α can be made assuming some hypothetical values for some of the variables in Equation 12. Assuming A = 60 mBq/m^3; QT_s = (4 Lh^{-1}) (170 h/month) x 10^{-3} = 0.68 m^3; $\delta\eta C_F \sim 0.01$; and S/S_T

~0.3; Equation 12 gives, assuming contamination arising from LLRD deposited on the collimator walls:

$$N'_{\alpha} \sim 25 \text{ tracks/collimator}$$

These figures could, of course, be much higher depending on the value of the combined variable $\delta\eta C_p$, which is unknown, but presumed to be substantially higher than the value of 1% (i.e., 0.01) used above.

The contamination problem discussed above is not only important because of the number of unwanted tracks recorded in the $^{218}Po/^{212}Bi$, ^{214}Po and ^{212}Po channels, but most importantly because of the channel(s) where these 'extra' tracks appear affect the calculation of WLM (see Equations 3 and 4) differently.

It should be noted that consistently higher values for the number of tracks in the ^{218}Po channel have been reported (18). This can only be explained by contamination of the sampling head. Furthermore, contamination of the sampling head has indirectly been evidenced by careful examination of the detector films where quite often dense and relatively large clusters of nuclear tracks have been found (15, 18)

Contamination by LLRD is a serious problem which should be avoided. Two immediate solutions to this problem come to mind, namely:

a) removing contamination after each monthly exposure;

b) designing a disposable sampling head.

Needless to say that a major redesigning of the dosimeter to eliminate the problem altogether, i.e., no leaks, would be preferable. However, it seems difficult from the practical standpoint as indicated elsewhere (18).

It should be born in mind that the above discussion is not only restricted to long-lived radioactive dust (LLRD), but can be extended to the radon and thoron progenies as well. Contamination by these radioactive products could be as important, or more important, than that of LLRD.

Equation 12 could also be applied in this case provided δ, η and C_F can be determined. Contributions from radon (thoron) progeny deposited on the collimator walls, due to air leaks, has not been adequately researched.

Another important consideration is the sensitivity limitation of the dosimeter which is partly determined by environmental conditions and the physical properties of the film detector.

The ultimate sensitivity of the dosimeter is limied by the background contribution to which the dosimeter is affected in a clean environment and with no air sampling. The background contribution arises from cosmic radiation that upon energy degradation can produce nuclear tracks in the film, and from the presence of natural radon, thoron and their progenies which diffuse into the sampling head of the dosimeters.

Typical examples for the dosimeters background have been measured by CAIRS (18,19). Two independent series of experiments, using 20 sampling heads each time, gave the following results:

$$\text{WLM(Rn)} = 0.018 \pm 0.01 \text{ and } 0.012 \pm 0.01, \text{ and}$$

$$\text{WLM(Tn)} = 0.011 \pm 0.02 \text{ and } 0.008 \pm 0.02.$$

The values given above are in some cases of the same order as the values reported for some dosimeters during ehe dosimetry program. In most cases, however, the background values are a significant contribution to the total radiation exposure, i.e., at least 10 to 20%.

Differences in film sensitivity from batch to batch have been observed, the reason for this not being clearly understood.

Some anomalies were also noted, i.e., some dosimeters were not worn for variable periods of time, but radiation exposures for these dosimeters were reported. However, upon close examination it was realized that these exposures were in fact of the same order of magnitude as the background readings reported above, i.e., from 0.0005 to 0.02 with a mean value of 0.011

for WLM(Rn), and from 0.001 to 0.04 with a mean value of 0.006 for WLM(Tn).

FINAL COMMENTS AND CONCLUSION

The data presented in this report show significant differences between radiation exposure determined by personal dosimetry and grab-sampling. A careful analysis of the results suggest the following as the most likely contribution to this disagreement:

1. Significant differences in flow rate for a given dosimeter when measured on a monthly basis.
2. Long-lived radioactive dust contamination of the dosimeter sampling head. However, contamination by radon and thoron progeny should not be excluded.
3. Dosimeter background which often represented a significant fraction of the total dosimeter reading under normal underground operating conditions.
4. Poor counting statistics of grab-samples, particularly at low Working Levels. The accuracy of grab-sampling measurements, as normally carried out, is expected to be about 10 to 20% at best, and in many cases of the order of 30%.
5. Overestimation of WL(Rn) due to the thoron progeny contribution counted as radon progeny. It is estimated that WL(Rn) has been consistently overestimated by about 15%.
6. It should be noted that in each case exposure times were assumed by CAIRS to be 170 h/month. Hence, individual radiation exposure in some cases could be affected by an error of up to one order of magnitude.

As previously indicated, personal dosimetry data have been consistently lower than grab-sampling data.

Perhaps the most significant experimental find in the dosimetry program is not the disagreement between radiation exposure evaluated by personal dosimetry and grab-sampling due to some systematic bias in the operational

procedures, methods and techniques used, but the poor correlation between these two radiation exposure data sets. This lack of correlation has also been indicated by other researchers (19).

Generally speaking, the usefulness of the personal dosimetry program has been somewhat limited because of items 1 to 6. There is litle doubt in the authors minds that substantially better agreement could have been attained had some improvements in the operational procedures been introduced. However, this could have only been accomplished at the expense of increased manpower requirements and the committment of more financial resources.

Perhaps the major benefit derived from the personal dosimetry program has been the experience gained in implementing and managing such a program. However, in its present format, agreement between grab-sampling data and personal dosimetry data cannot be expected to be better than within about 50% at best.

It is not altogether clear from the experimental data obtained, and the discussions above, which of the two radiation exposure methods provides a better, or more accurate, description of personal exposure levels of occupational workers in underground uranium mines. It is hoped that the analysis of data from two other mines, i.e., Stanleigh and Panel Mines will shed some additional light on personal dosimetry in Canadian mines.

ACKNOWLEDGEMENTS

The authors would like to thank Dr. E. Becker (CAIRS) for supplying some information and clarifying some points in the course of writing this report.

REFERENCES

1. McCurdy, D.E., "Thermoluminescent dosimetry for monitoring of uranium mines"; USAEC Report COO-1500-16; Colorado State University, Fort Collins, Colorado; June 1969.

2. McCurdy, D.E., Schiager, K.J. and Flack, E.D., "Thermoluminescent dosimetry for personal monitoring of uranium miners"; Health Physics, vol. 17, p. 414; 1969.

3. White, O. Jr., "An evaluation of six radon dosimeters"; USAEC Health and Safety Laboratory Technical Memorandum 69-23; October 1969. "Evaluation of MIT and ORNL radon daughter dosimeters"; USAEC Health and Safety Laboratory Technical Memorandum 70-3; July 1970. "Evaluation of MOD and ORNL radon daughter dosimeters"; USAEC Health and Safety Laboratory Technical Memorandum 71-17; October 1971.

4. Rock, L.R., "Measurement of employee's individual cumulative exposures to radon daughters as practiced in the United States"; Personal Dosimetry and Area Monitoring Suitable for Radon and Daughter Products; Proc of the NEA Special Meeting, Elliot Lake, Ontario, Canada; pp 71-90; 1976.

5. Breslin, A.J., "MOD working level dosimeter"; Personal Dosimetry and Area Monitoring suitable for radon and daughter products"; Proc. of the NEA Special Meeting, Elliot Lake, Ontario, Canada; pp 91-100; 1976.

6. Chapuis, A.M., See for instance "Dosimetry in French uranium mines"; Presented at a meeting on Personal Dosimetry and Personal Exposure Estimation, Ottawa, Ontario, October 5th 1978, sponsored by AECB.

7. Durkin, J., "An electronic instrument for radon daughter dosimetry"; Report of Investigation 8255, U.S. Bureau of Mines, 1977. See also Health Physics, vol 37, pp. 858-864; 1979.

8. Duport, P., Chapuis, A.M. and Pradel, J., "Appareil individuel pour la dosimetrie des descendants du radon"; In: Advances in Radiation Protection Monitoring; IAEA-SM-229/90, pp. 435-443; Vienna, 1979.

9. Yourt, G.R., "Field test of TLD Working Level dosimeters using H & H Custom Work and DuPont pumps fitted with ERDA-MOD dosimeter heads"; Report submitted to AECB in compliance with contract.

10. Bigu, J. and Regan, R., "A preliminary technical evaluation of the α-NUCLEAR electronic personal dosimeter in an underground uranium mine"; Division Report MRP/MRL 80-120(TR); CANMET, Energy, Mines and Resources Canada; August 1980.

11. Bigu, J. and Regan, R., "A technical evaluation of the U.S.B.M. personal (α-particle) dosimeter in an underground uranium mine"; Division Report MRP/MRL 81-8(CF); CANMET, Energy, Mines and Resources Canada; September 1980. (See also Durkin, J., U.S.B.M. RI 8255 and Health Physics, vol. 37, pp 757-764. 1979.)

12. Tremblay, R.J., Carson, D.W., Townsend, M.G., Bigu, J. and Regan, R., "A preliminary report on the evaluation of personal alpha dosimeters; flow rate measurement in a mine"; Division Report MRP/MSL 80-114(TR); CANMET, Energy, Mines and Resources Canada; August 1980.

13. Bigu, J. and Carson, D.W., "A preliminary report on the combined radon daughter/dust sampler (TLD/CAMPED) dosimeter"; Division Report MRP/MRL 79-63(TR); CANMET, Energy, Mines and Resources Canada; May 1979.

14. Parkinson, R.N., Roze, V. and Shepherd, R., "The development and underground testing of the alphaDOSIMETER - a solid state electronic personal radiation dosimeter for uranium mines"; In: Radiation Hazards in Mining - Control, and Medical Aspects, Manuel Gomez (Ed.) SME-AIME, pp 428-438, Kingsport Press Inc., Kingsport, Tennessee; 1981.

15. Bigu, J., Tremblay, R.J., Carson, D.W. and Townsend, M.G., "A technical evaluation of several personal α-dosimeters in Canadian uranium mines"; Division Report MRP/MRL 82-76(TR), CANMET, Energy, Mines and Resources Canada; March 1982.

16. Kusnetz, H.L., "Radon daughters in mine atmospheres"; Am Ind Hyg Assoc J,

vol 17, p 1; 1956. See also Ind Hyg Quarterly, March 1956.

17. Bigu, J., "Theoretical models for determining ^{222}Rn and ^{220}Rn progeny levels in Canadian underground uranium mines - a comparison with experimental data"; Health Physics, vol 48, No. 4, pp 371-399; 1985.

18. Becker, E., (CAIRS), private communication.

19. Duport, P., (AECB), private communication.

Table 1 - Air flow rate data for some dosimeters.

Dosimeter Number	Period	Flow rate (Q) Range L/h	$\overline{Q}\pm\sigma_Q$ L/h	Q_{max}/Q_{min}	$Q_{max}/\overline{Q}$	$Q_{min}/\overline{Q}$	$\left(\frac{\sigma_Q}{\overline{Q}}\right)x10^2$
42	Feb. 83/June 85	3.38-4.65	4.04±0.41	1.38	1.15	0.84	10.1
94	"	3.00-5.22	3.88±0.68	1.74	1.34	0.77	17.5
29	"	2.73-5.24	3.88±0.71	1.92	1.35	0.70	18.3
All (75 units)	"	3.33-4.44	3.99±0.37	1.33	1.11	0.83	9.3

Note: Q_{min} and Q_{max} stand, respectively, for minimum and maximum flow rate measured during the period indicated.

Table 2 - Dosimeter flow rate data.

Dosimeter Number	Q_{max} L/h	Q_{min} L/h	$\bar{Q}\pm\sigma_Q$ L/h	Q_{max}/Q_{min}	$(\sigma_Q/\bar{Q})\times10^2$**
26	3.84	3.23	3.65	1.19	
27	3.36	3.00	3.17	1.12	
28	3.62	3.00	3.32	1.21	
29	3.14	2.70	2.95	1.16	
30	4.00	3.51	3.70	1.14	
31	4.25	3.60	3.96	1.18	
32	4.38	3.63	4.00	1.21	
33	3.91	2.43	3.50	1.61*	
34	3.60	2.85	3.33	1.26	
35	3.85	3.16	3.55	1.22	
36	4.08	3.18	3.65	1.28	
37	3.66	3.00	3.37	1.22	
38	4.00	3.54	3.73	1.13	
39	4.30	2.63	3.24±0.51**	1.63*	15.8
40	3.72	2.79	3.14	1.33	
41	3.39	3.03	3.21	1.12	
42	4.00	3.08	3.61	1.30	
43	3.60	2.73	3.13	1.32	
44	3.95	3.00	3.52	1.32	
45	4.28	3.51	3.55	1.22	
46	4.00	3.29	3.88	1.21	
47	3.63	2.40	3.11±0.42**	1.51*	13.5
48	3.76	3.06	3.48	1.23	
49	4.98	3.96	4.43	1.26	
50	4.31	3.66	4.00	1.18	
51	4.11	3.81	3.99	1.08	
52	4.65	4.31	4.49	1.08	
53	5.04	3.83	4.22	1.32	
54	4.20	3.84	3.96	1.09	
55	4.38	3.00	3.32±0.44**	1.46*	13.2
56	4.51	3.73	4.17±0.26**	1.21*	6.2
57	4.08	3.45	3.80	1.18	
58	4.20	3.40	3.82	1.23	
59	3.85	2.89	3.34	1.33	
60	3.59	3.40	3.90	1.06	
61	4.21	3.54	3.90	1.19	
62	4.81	4.10	4.36	1.17	
63	3.78	3.33	3.53	1.13	
64	4.71	4.08	4.30	1.15	
65	4.10	3.00	3.75	1.37	
66	4.25	3.24	3.85	1.31	
67	4.20	3.75	3.99	1.12	
68	4.32	3.67	4.03	1.18	
69	3.93	3.06	3.59	1.28	
70	5.28	4.23	4.82	1.25	
71	5.34	3.90	4.21	1.37	
72	3.90	3.60	3.74	1.08	
73	4.02	3.18	3.62	1.26	
74	4.18	2.46	3.57	1.70*	
75	4.28	3.40	3.81	1.26	
76	3.79	3.00	3.36±0.22**	1.26	6.5
77	4.30	2.45	3.81	1.75*	
78	3.81	3.23	3.58	1.18	
79	4.29	2.86	3.63±0.44**	1.50*	12.1
80	4.14	3.27	3.61	1.27	
81	4.56	3.91	4.30	1.17	
82	4.38	4.00	4.18	1.09	
83	4.68	3.96	4.37	1.18	
84	3.98	3.00	3.61	1.33	
85	4.13	3.60	3.89	1.15	
86	4.38	3.81	4.04	1.15	
87	4.20	3.30	3.85	1.27	
88	3.48	3.00	3.17	1.16	
89	4.56	3.48	4.07	1.31	
90	4.65	4.03	4.37	1.15	
91	3.67	3.21	3.51	1.14	
92	3.71	2.94	3.31	1.26	
93	3.63	3.00	3.34	1.21	
94	4.17	3.48	3.79	1.20	
95	-	-	-	-	
96	3.38	2.73	3.14	1.24	
97	-	-	-	-	
98	3.91	3.69	3.81	1.06	
99	4.10	3.00	3.73	1.37	
100	4.20	3.89	4.01	1.08	
		Ave:	3.73 ± 0.38		

* Asterisks indicate ratios larger than 1.40

** $\sigma_{\bar{Q}}$ is the standard deviation of the mean.

Table 3 - $(WLM)_{DOS}$ and $(WLM)_{T,GS}$ percentage distributions within some Working Level Month intervals*.

Year	$(WLM)_{DOS}$ Range	Percentage (%)	Total Percentage (%)	Year	$(WLM)_{T,GS}$ Range	Percentage (%)	Total Percentage (%)
1983	0-0.05	41.7		1983	0-0.05	11.8	
	0.05-0.1	28.6			0.05-0.1	25.0	
	0.1-0.15	16.6	86.9		0.1-0.15	31.8	
					0.15-0.2	15.4	84.0
1984	0-0.05	26.0					
	0.05-0.1	29.9		1984	0-0.05	8.7	
	0.1-0.15	18.3			0.05-0.1	26.8	
	0.15-0.2	11.8	86.0		0.1-0.15	31.0	
					0.15-0.2	20.0	86.5
1985	0-0.05	13.1					
	0.05-0.1	31.0		1985	0-0.05	8.5	
	0.1-0.15	22.5			0.05-0.1	18.8	
	0.15-0.2	14.6	81.2		0.1-0.15	27.7	
					0.15-0.2	25.3	80.3

* Percentages corresponding to WLM >0.2 are not included in this Table.

Table 4 - Linear regression analysis data pertaining to several occupational codes (see Figures 18 to 23).

Occupation	Occupation Code	Slope (m)	Intercept (b)	Correlation Coeff., σ	Year
Driller	230	0.6169	0.1024	0.564	1983
"	"	0.0017	0.1327	0.049	1984
"	"	0.6492	0.0912	0.417	1985
Slusherman	228	0.5801	0.073	0.719	1983
"	"	0.0835	0.1529	0.094	1984
"	"	-0.3126	0.2453	-0.191	1985
Diamond Driller	227	0.2301	0.099	0.226	1983
" "	"	0.4303	0.070	0.464	1984
" "	"	0.0928	0.100	0.0982	1985
Timberman	220	0.1659	0.1261	0.2924	1983
"	"	0.2004	0.1127	0.380	1984
"	"	0.9795	0.0042	0.711	1985
Level Serviceman	211	0.3573	0.0634	0.554	1983
" "	"	0.0557	0.0915	0.069	1984
" "	"	0.2769	0.0822	0.371	1985
Mine Shift Boss	994	0.2960	0.0930	0.436	1983
" " "	"	0.1105	0.1273	0.216	1984
" " "	"	0.4009	0.0931	0.641	1985

Note: data fitted to a straight line of the form:

$$(WLM)_{T,GS} = m(WLM)_{DOS} + b$$

Table 5 - Linear regression analysis data pertaining to all occupational codes during the period 1983 to 1985.

Occupational Code	Slope (m)	Intercept (b)	Correlation Coeff., σ
207	0.6235	0.0629	0.4571
208	-0.0142	0.1826	-0.0223
209	-0.3869	0.1138	-0.2019
210	0.0696	0.0443	0.1608
211	0.2541	0.0768	0.3774
213	0.3255	0.1133	0.4773
214	0.2596	0.1449	0.5295
215	1.2099	0.0782	0.4645
216	0.5807	0.0934	0.7150
217	0.4723	0.1018	0.6052
218	0.0116	0.1591	0.0178
219	0.1999	0.1499	0.2774
220	0.2247	0.1176	0.3684
221	0.2004	0.0950	0.2199
227	0.2699	0.0896	0.2775
228	0.1165	0.1522	0.1451
230	0.6333	0.0884	0.5427
231	0.0668	0.1417	0.1619
232	0.2106	0.1131	0.3922
234	-0.2719	0.1030	-0.5370
236	0.1189	0.0928	0.1102
237	0.3313	0.0781	0.3754
238	0.1615	0.0856	0.2002
240	0.2283	0.1408	0.1279
244	0.0929	0.2571	0.0863
402	-0.1260	0.1315	-0.2493
436	0.0633	0.1331	0.1773
505	0.0081	0.1409	0.0221
540	1.1993	0.0424	0.7818
541	0.1893	0.1239	0.2717
555	0.8467	0.0394	0.7828
574	0.2015	0.1217	0.2516
591	0.1280	0.0558	0.2073
592	0.0079	0.0461	0.0828
651	-0.0157	0.0442	-0.0337
652	4.0977	-0.4008	0.5636
967	0.1294	0.0874	0.1518
970	0.4414	0.0837	0.6021
992	0.2270	0.0292	0.4118
994	0.2134	0.1082	0.3801

Note: data fitted to a straight line of the form:

$$(WLM)_{T,GS} = m\ (WLM)_{DOS} + b$$

Table 6 - Linear regression analysis data pertaining to all dosimeters (see Figures 24 to 26).

Year	Slope (m)	Intercept (b)	Correlation Coeff., σ
1983	0.3403	0.1013	0.3995
1984	0.2930	0.099	0.380
1985	0.4014	0.1009	0.3596

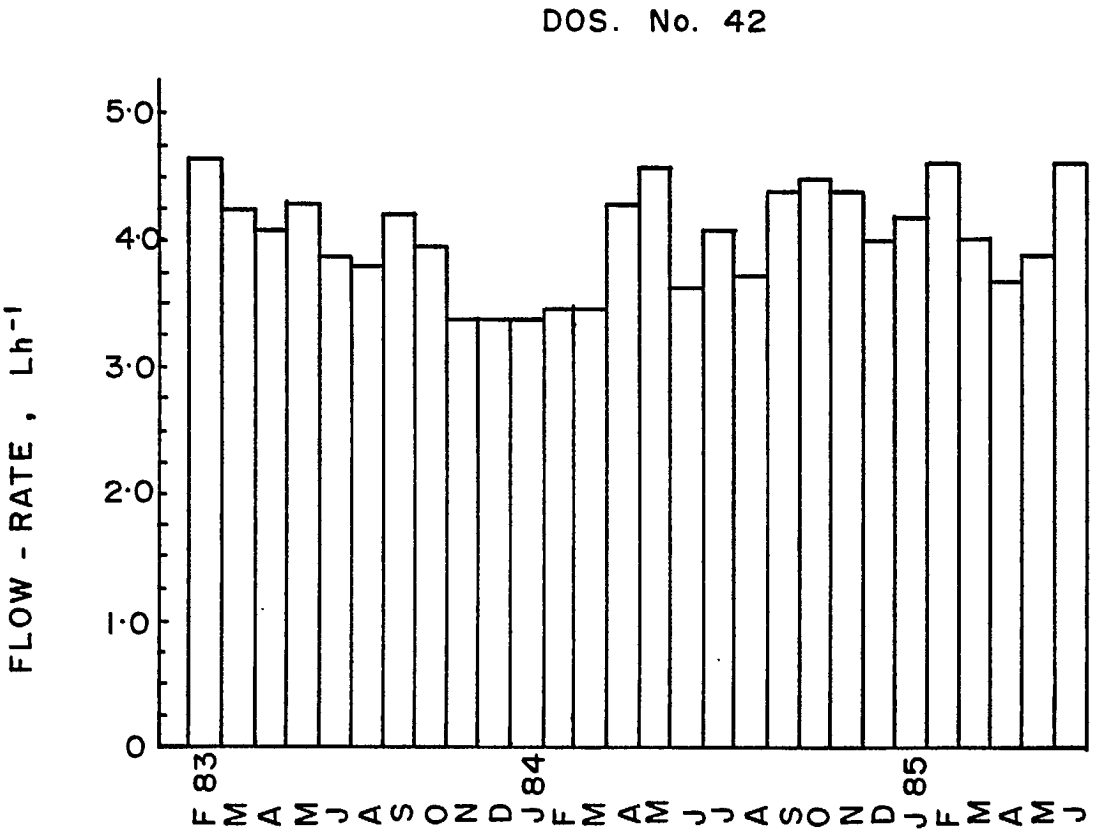

Fig. 1 - Flow rate versus time for dosimeter No. 42.
Time axis shows the month and year (abbreviated).

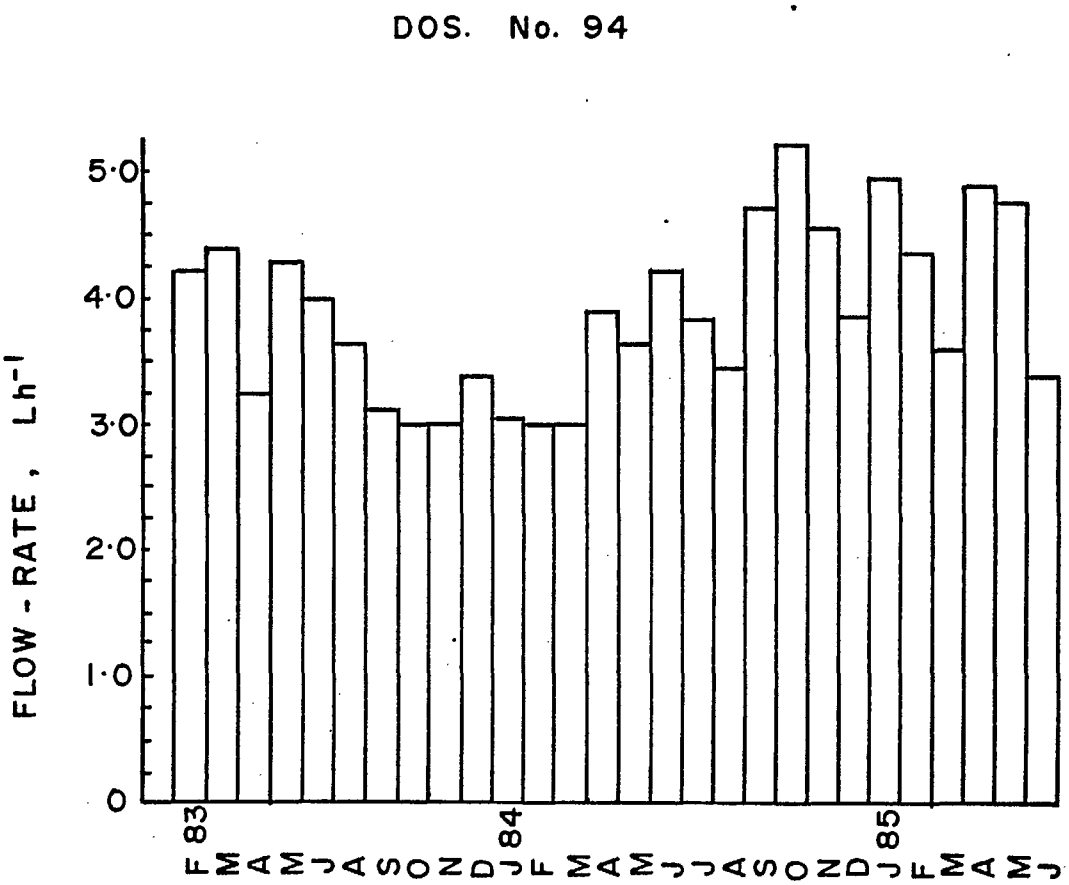

Fig. 2 - Flow rate versus time for dosimeter No. 94. Time axis shows the month and year (abbreviated).

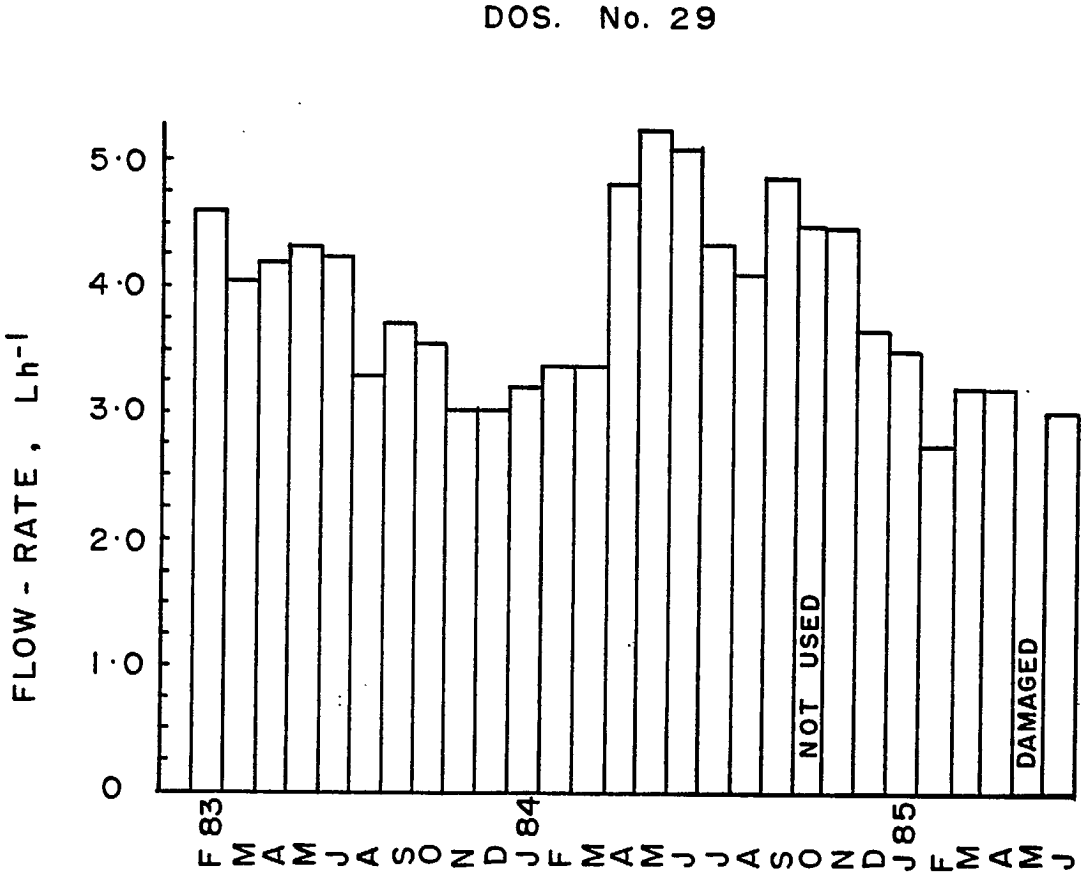

Fig. 3 - Flow rate versus time for dosimeter No. 29. Time axis shows the month and year (abbreviated).

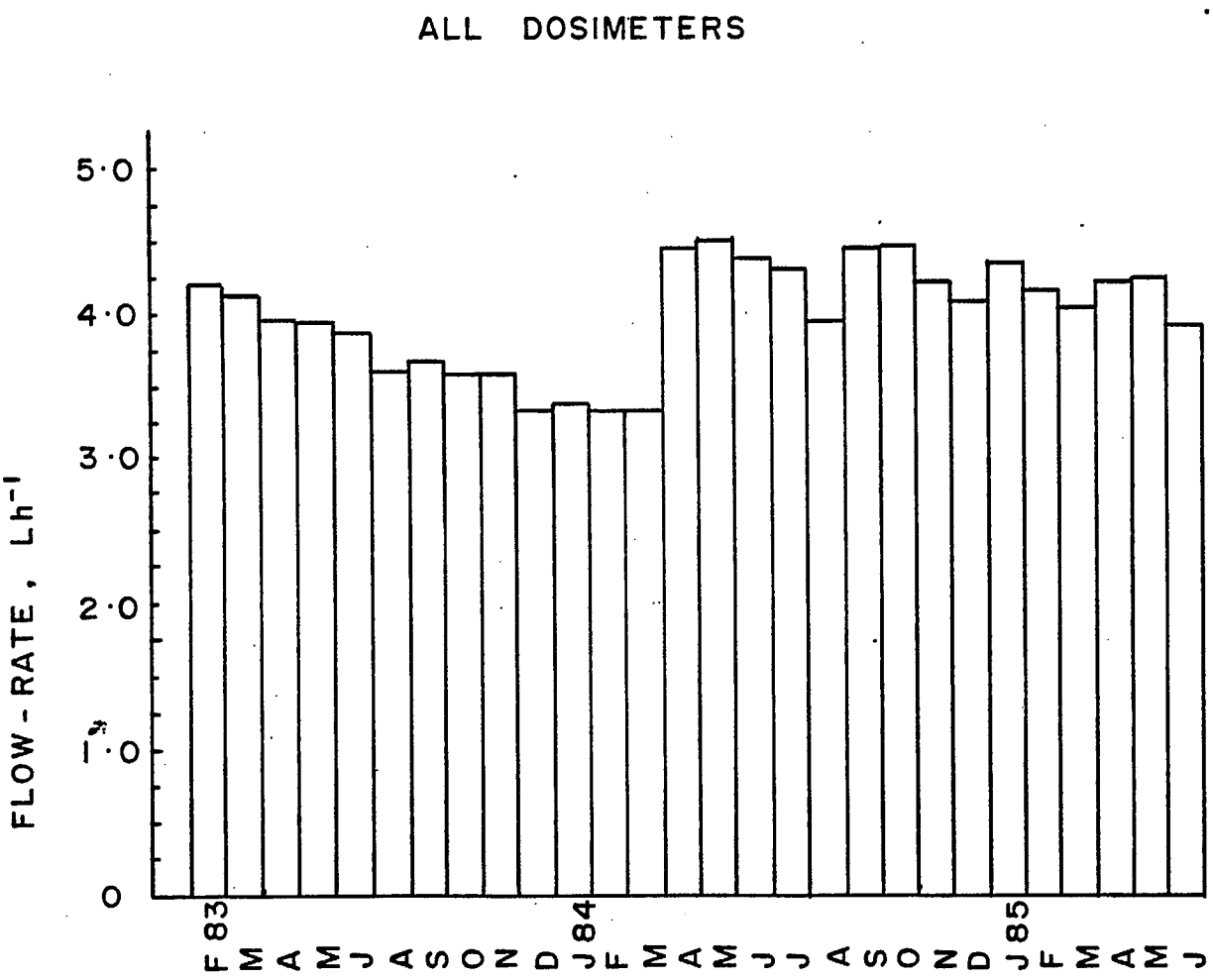

Fig. 4 - Average flow rate for all dosimeters combined versus time. Time axis shows the month and year (abbreviated).

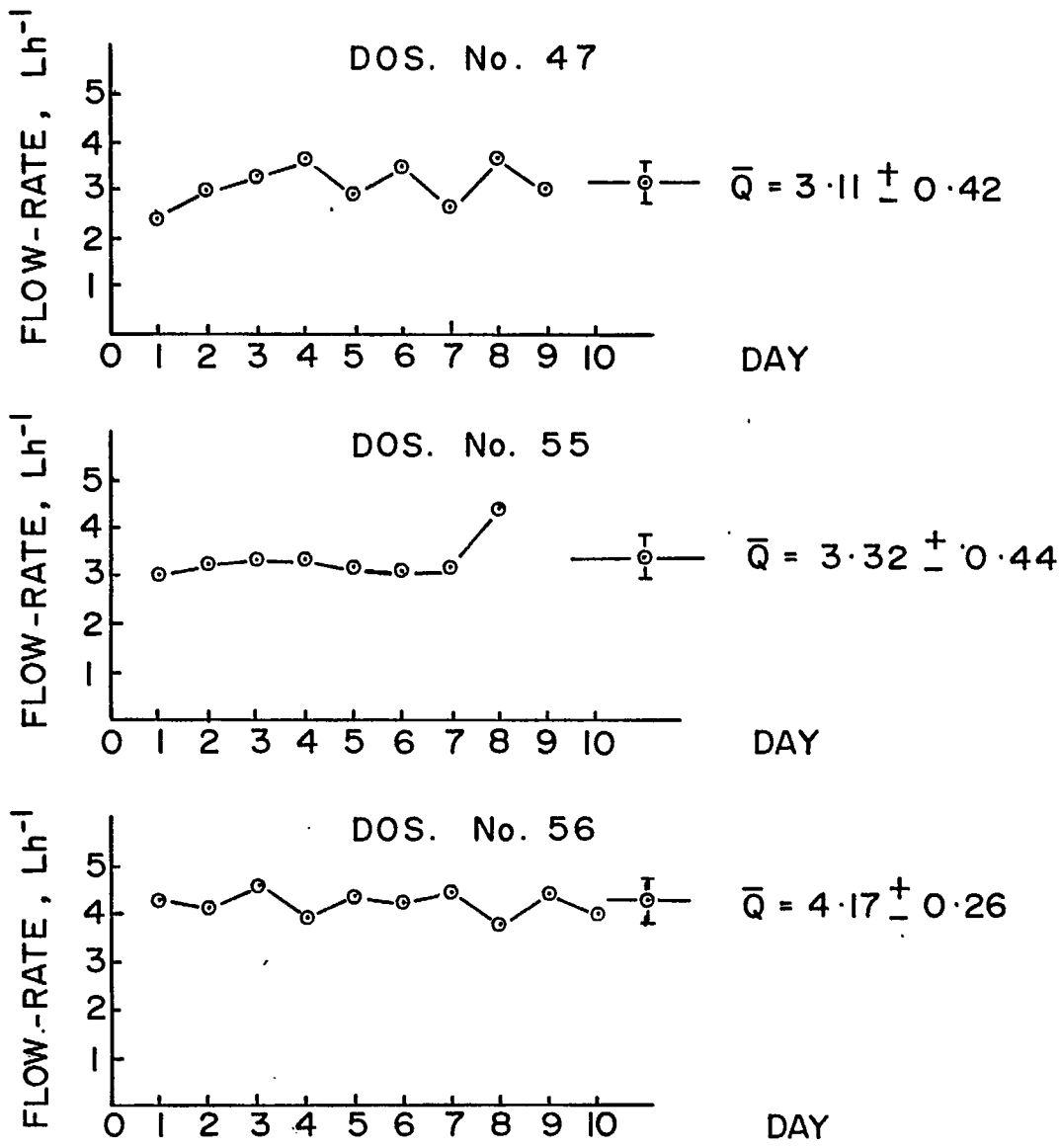

Fig. 5 - Daily average flow rate versus time for several dosimeters.

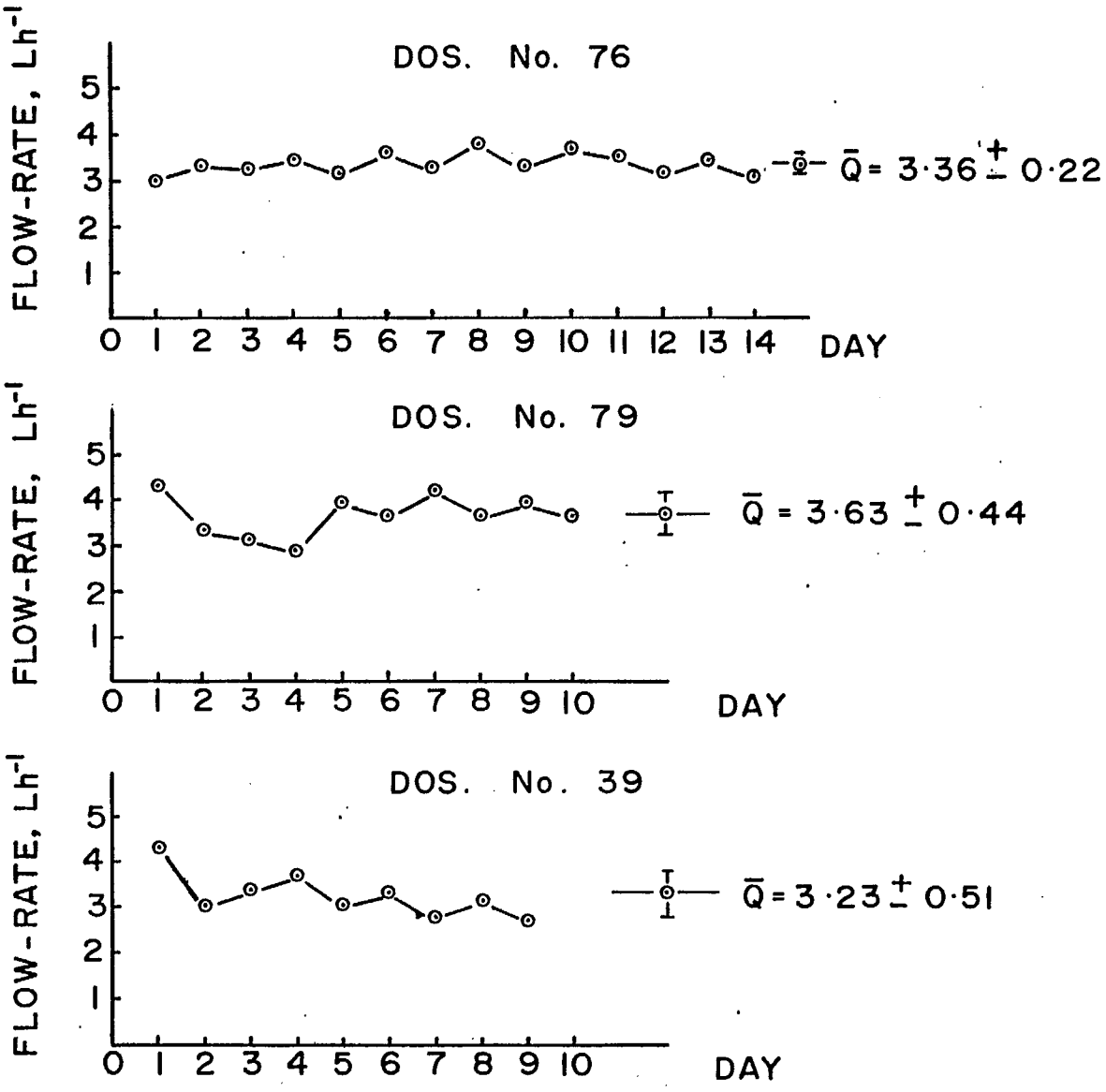

Fig 6 - Daily average flow rate versus time for several dosimeters.

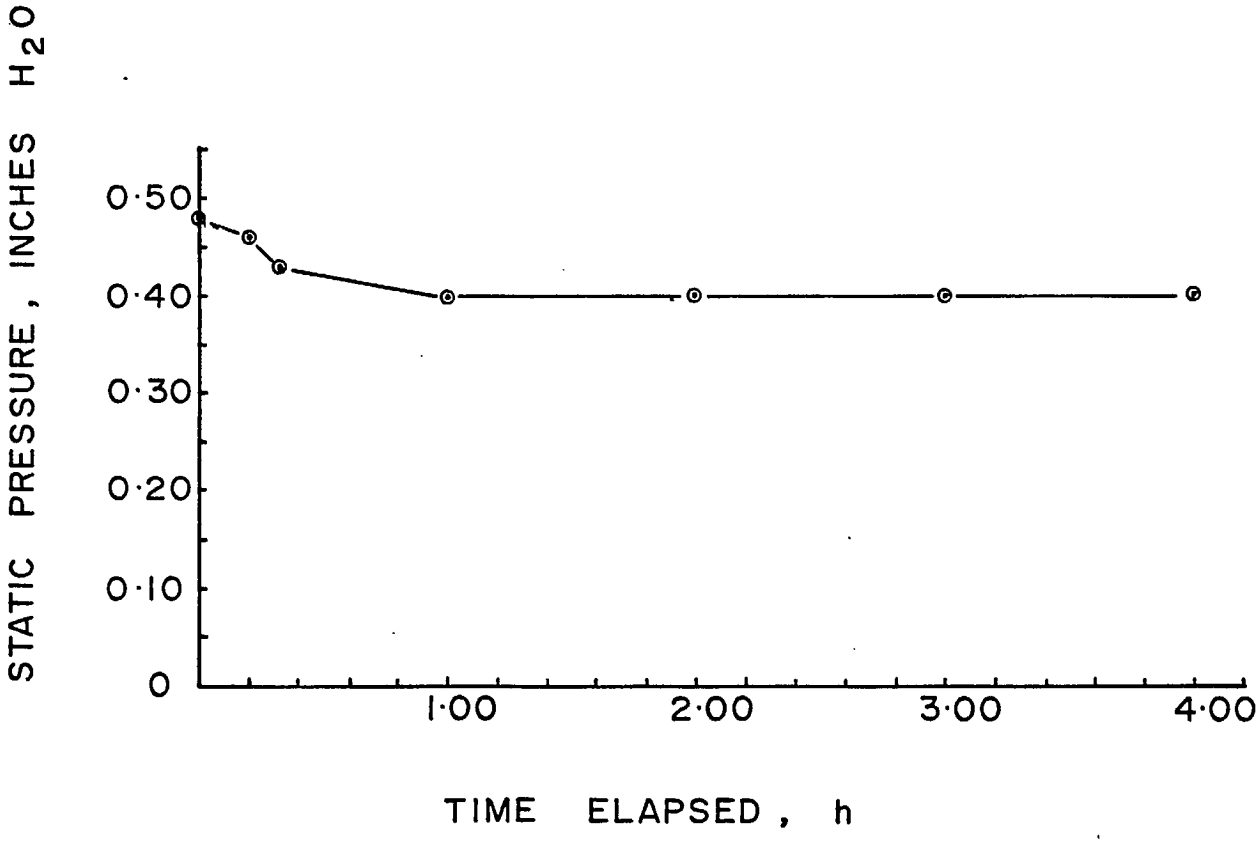

Fig. 7 - Dosimeter pump static pressure versus time.

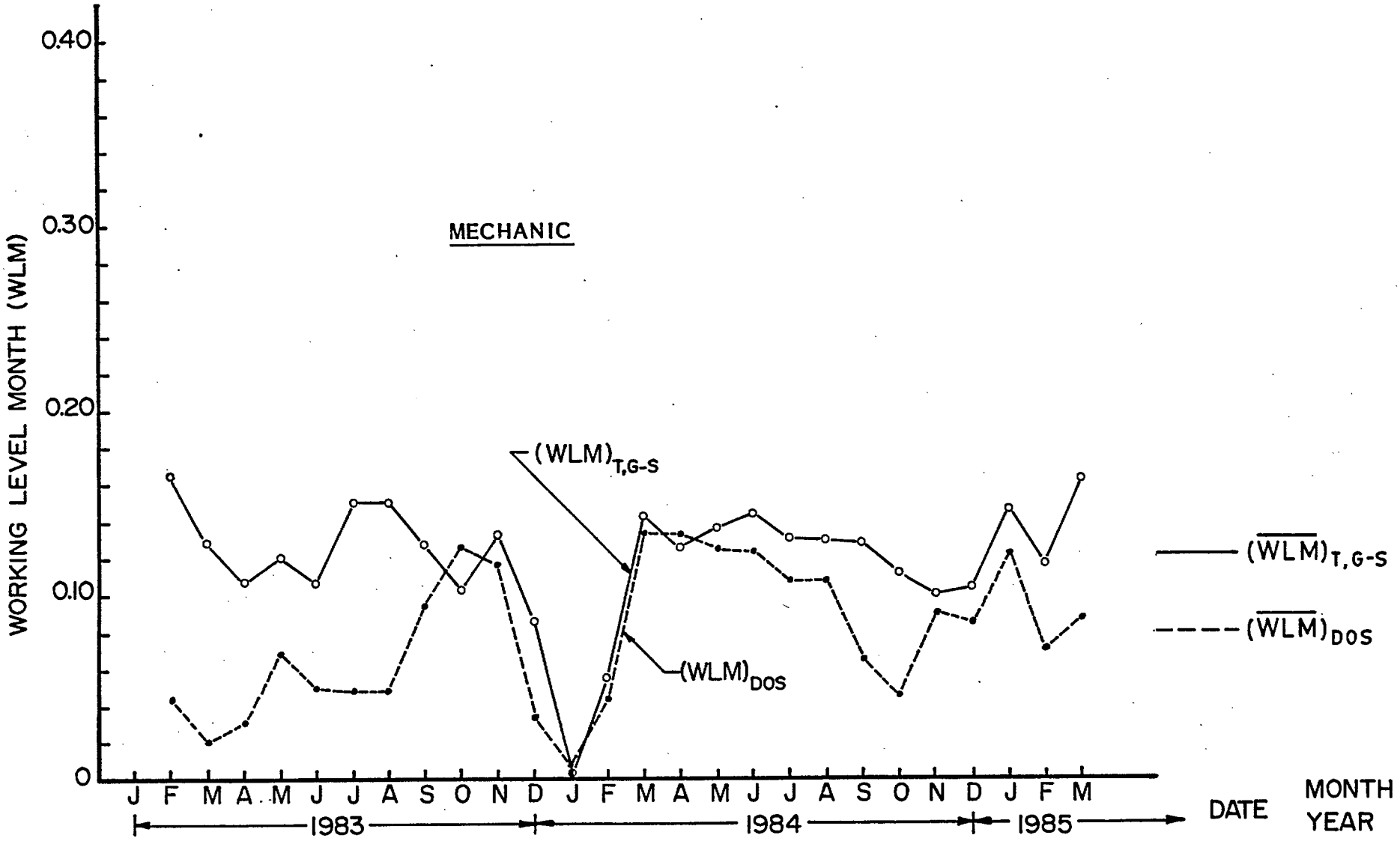

Fig. 8 - Working Level Month versus time. Also shown is the average value.

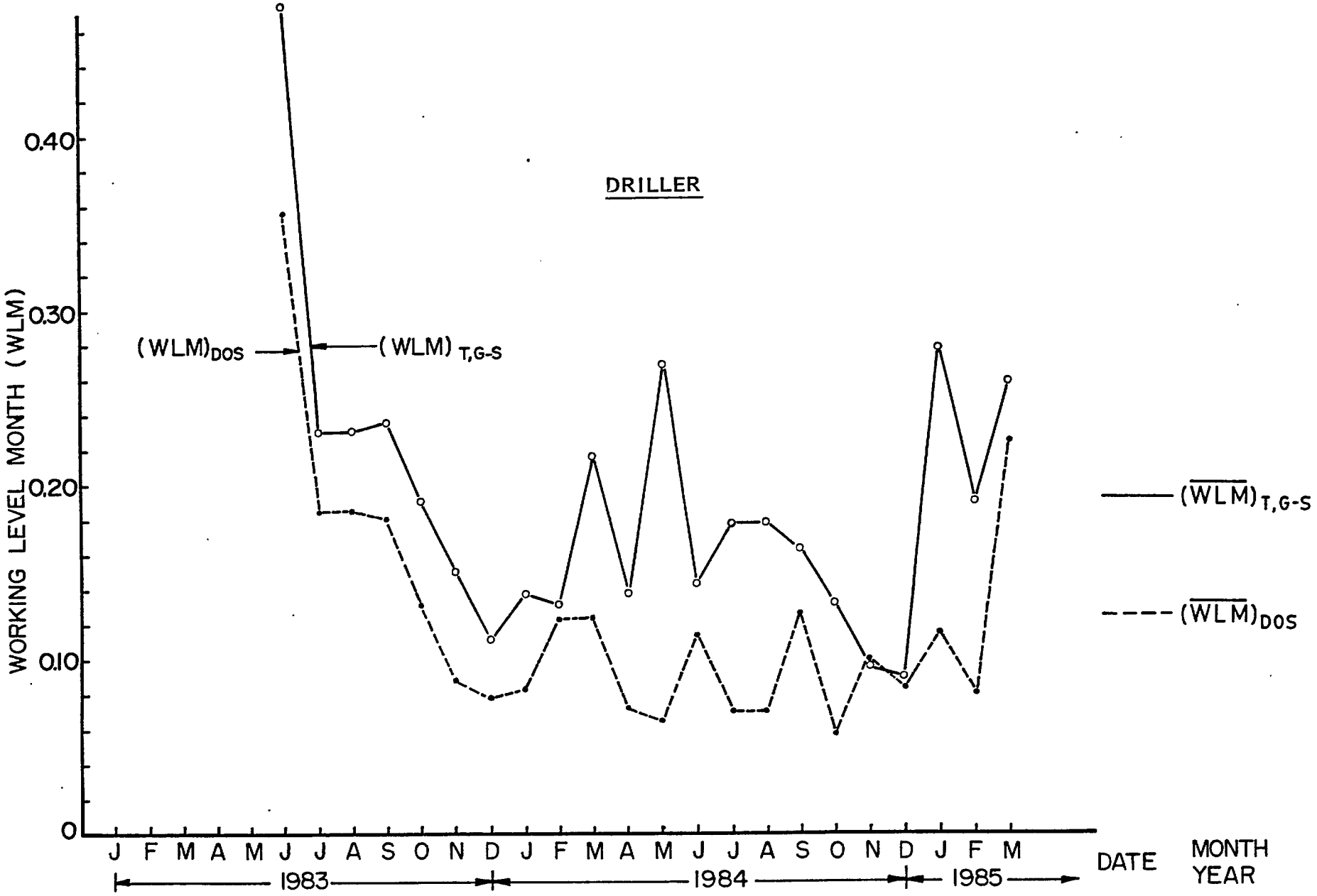

Fig. 9 - Working Level Month versus time. Also shown is the average value.

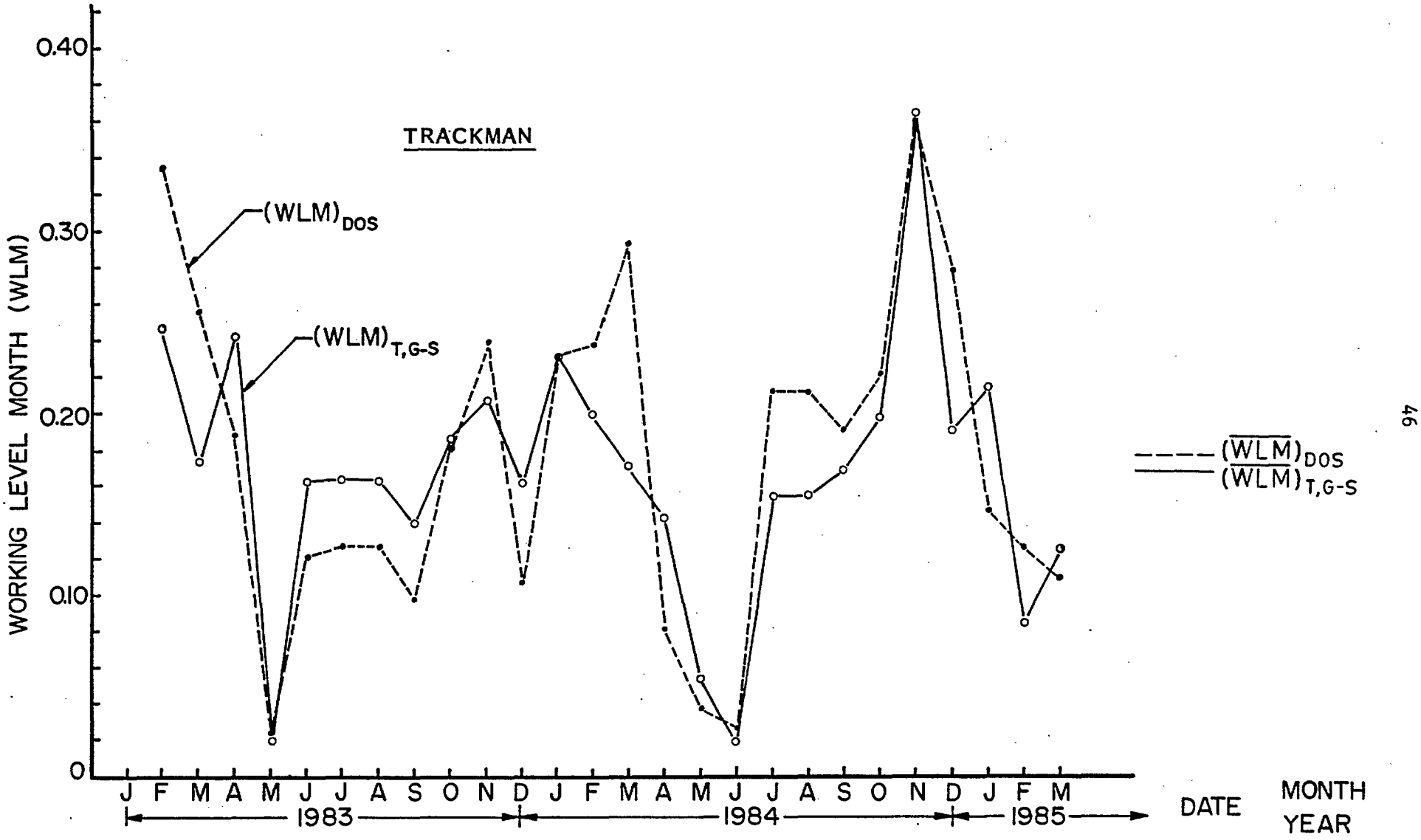

Fig. 10 - Working Level Month versus time. Also shown is the average value.

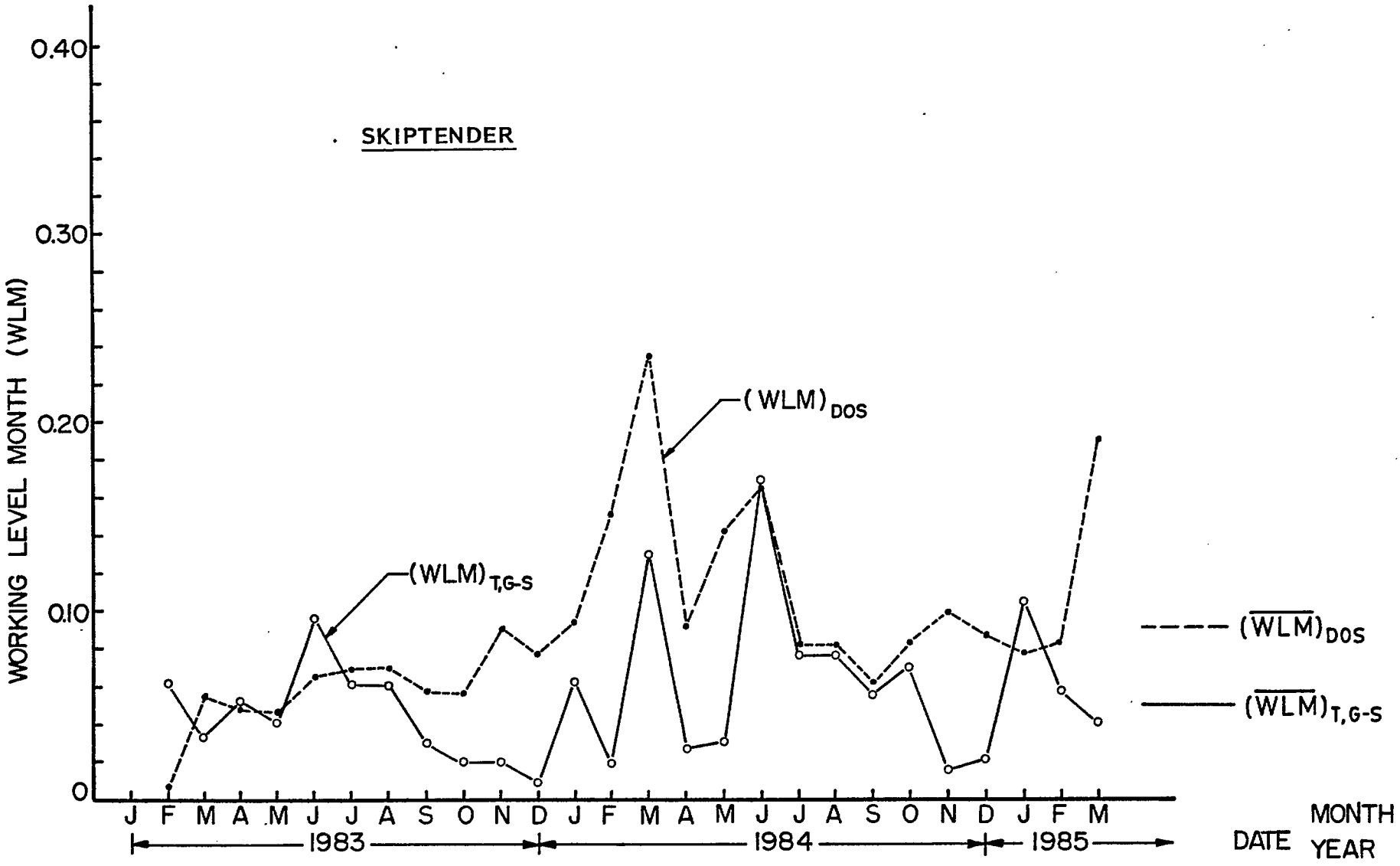

Fig. 11 - Working Level Month versus time. Also shown is the average value.

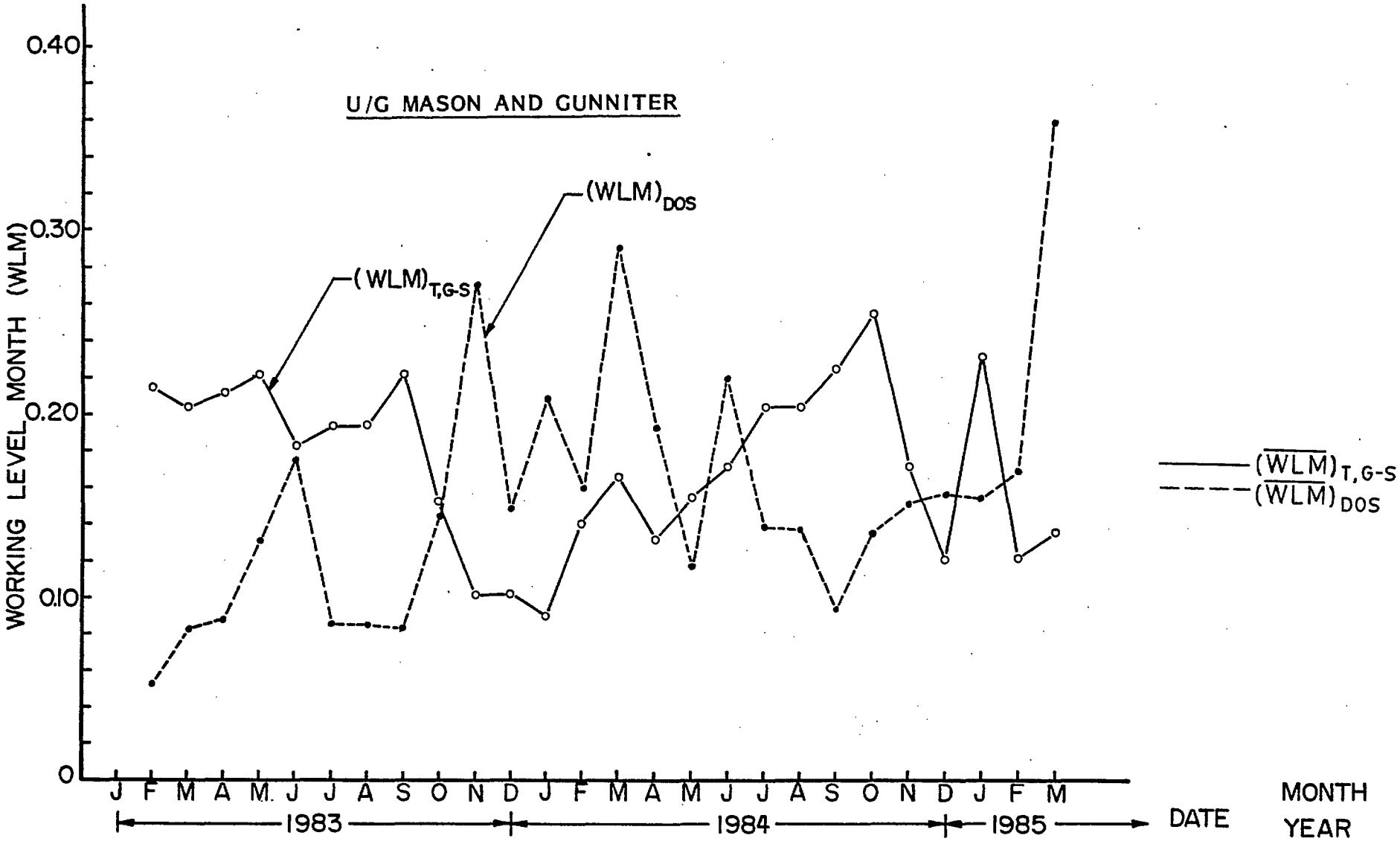

Fig. 12 - Working Level Month versus time. Also shown is the average value.

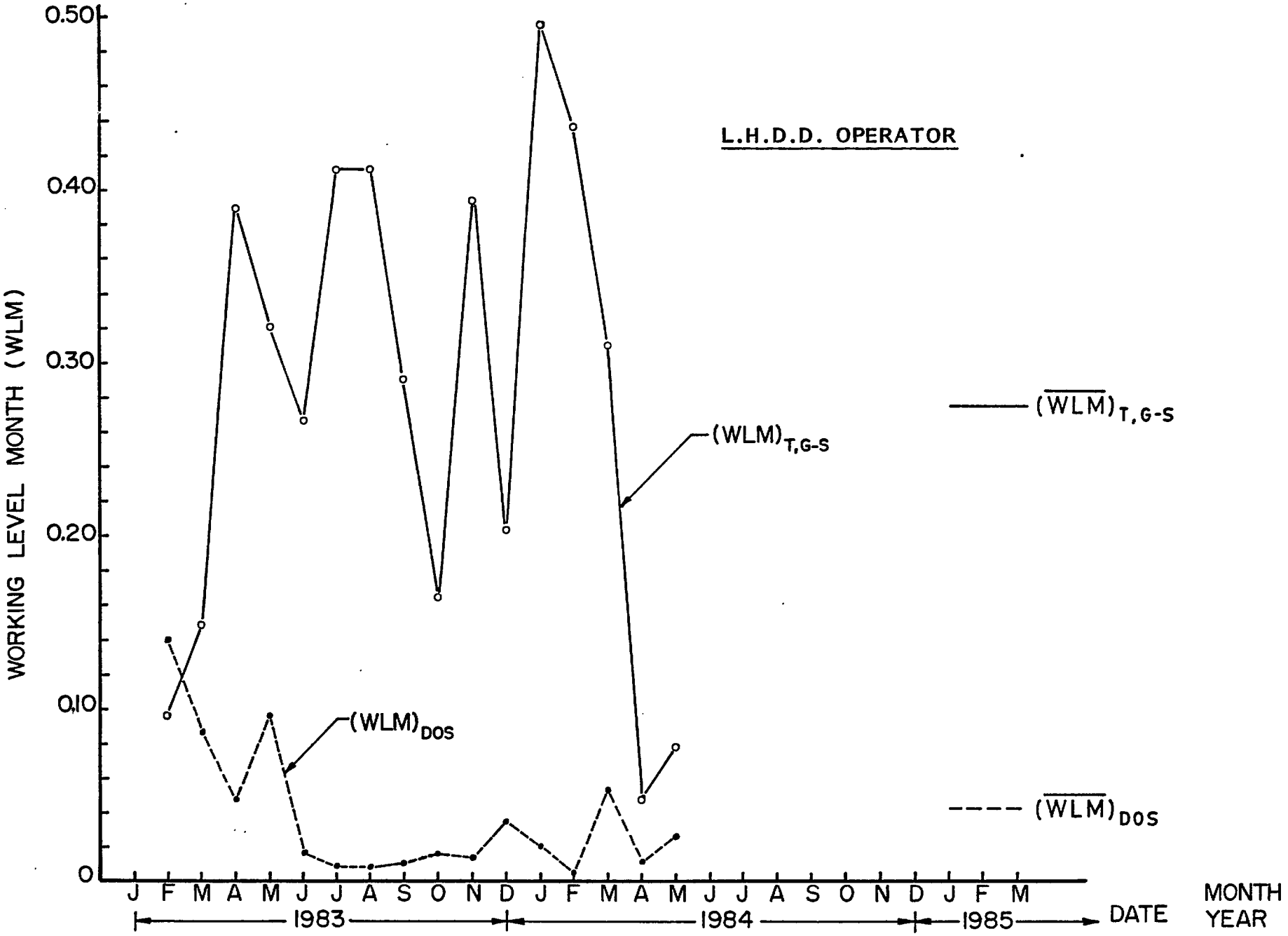

Fig. 13 - Working Level Month versus time. Also shown is the average value.

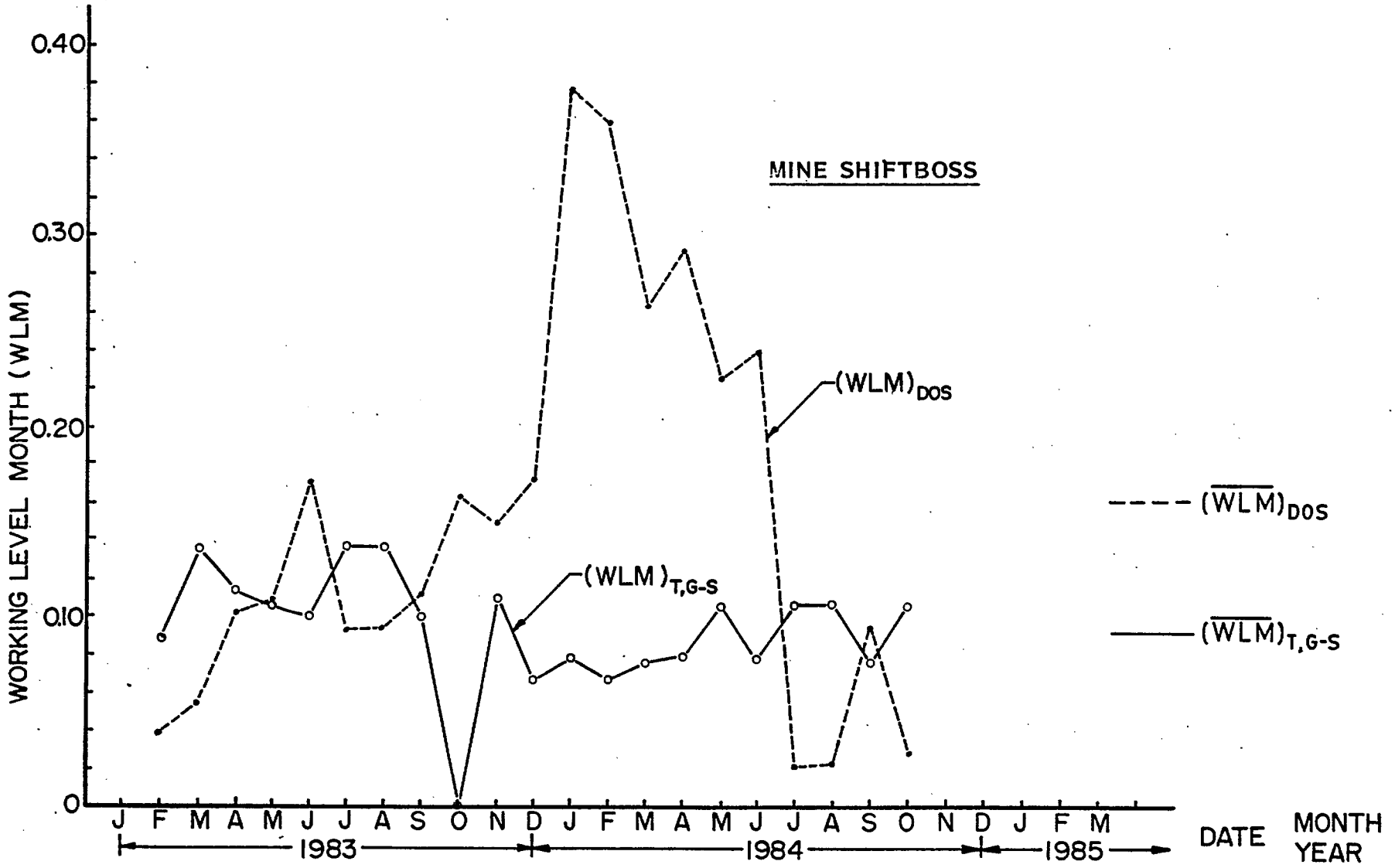

Fig. 14 - Working Level Month versus time. Also shown is the average value.

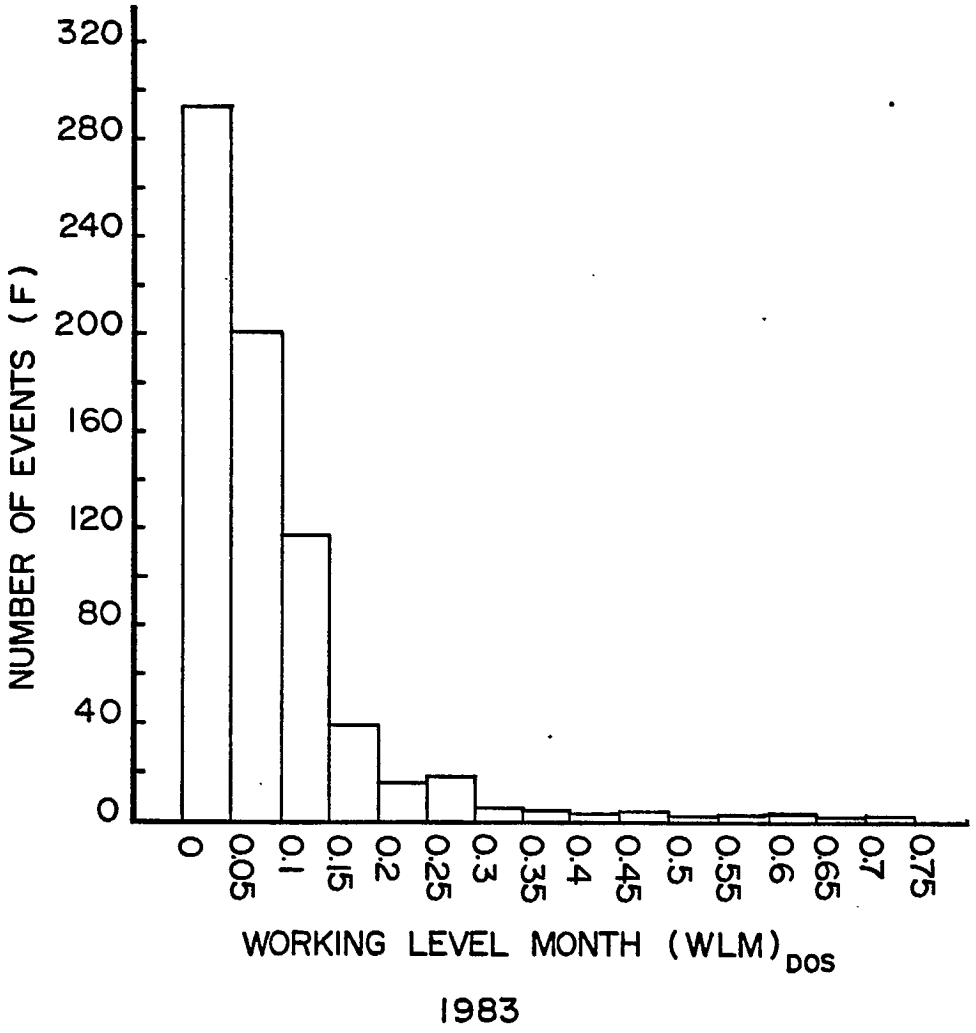

Fig. 15 - Working Level Month frequency distribution.

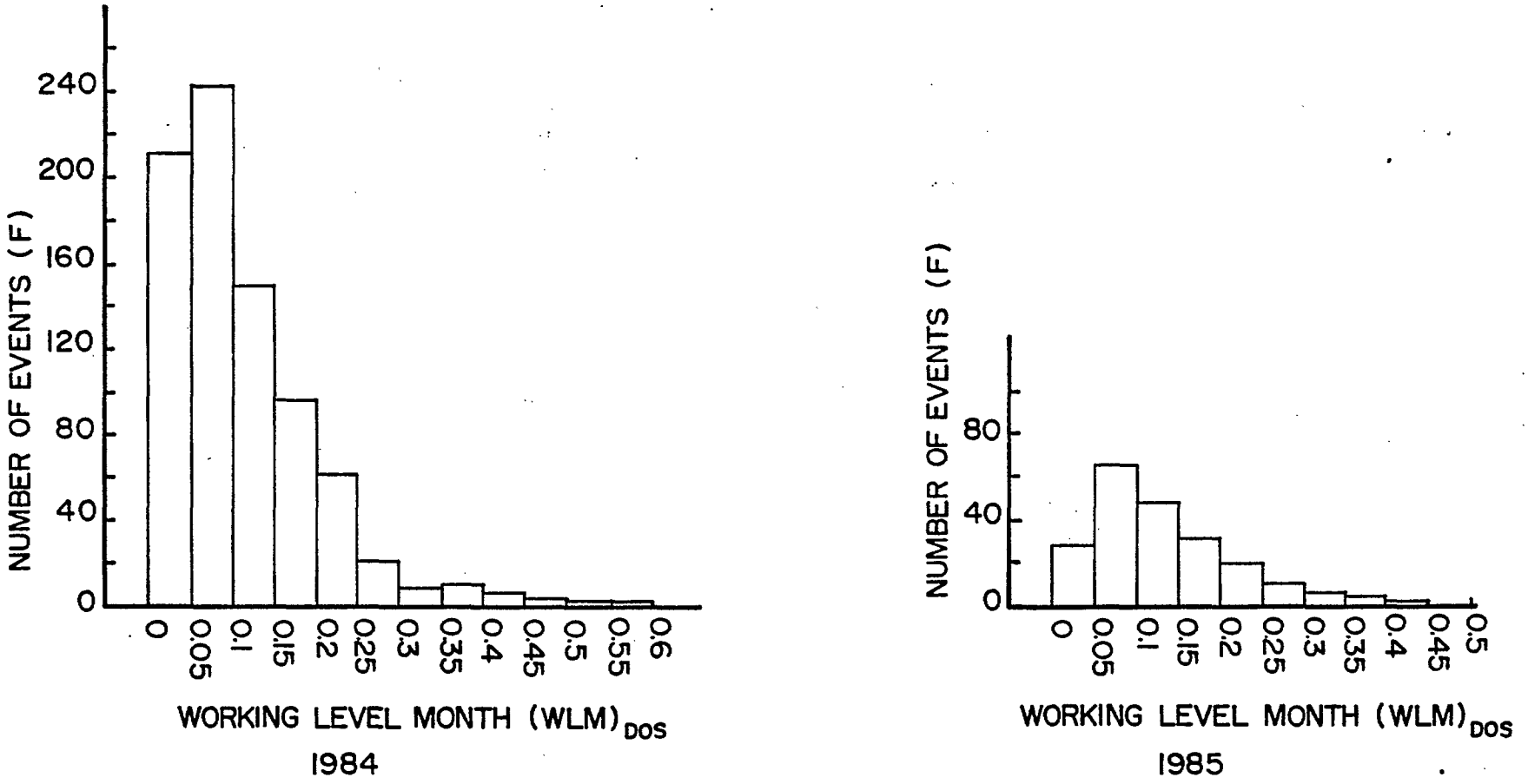

Fig. 16 - Working Level Month frequency distribution.

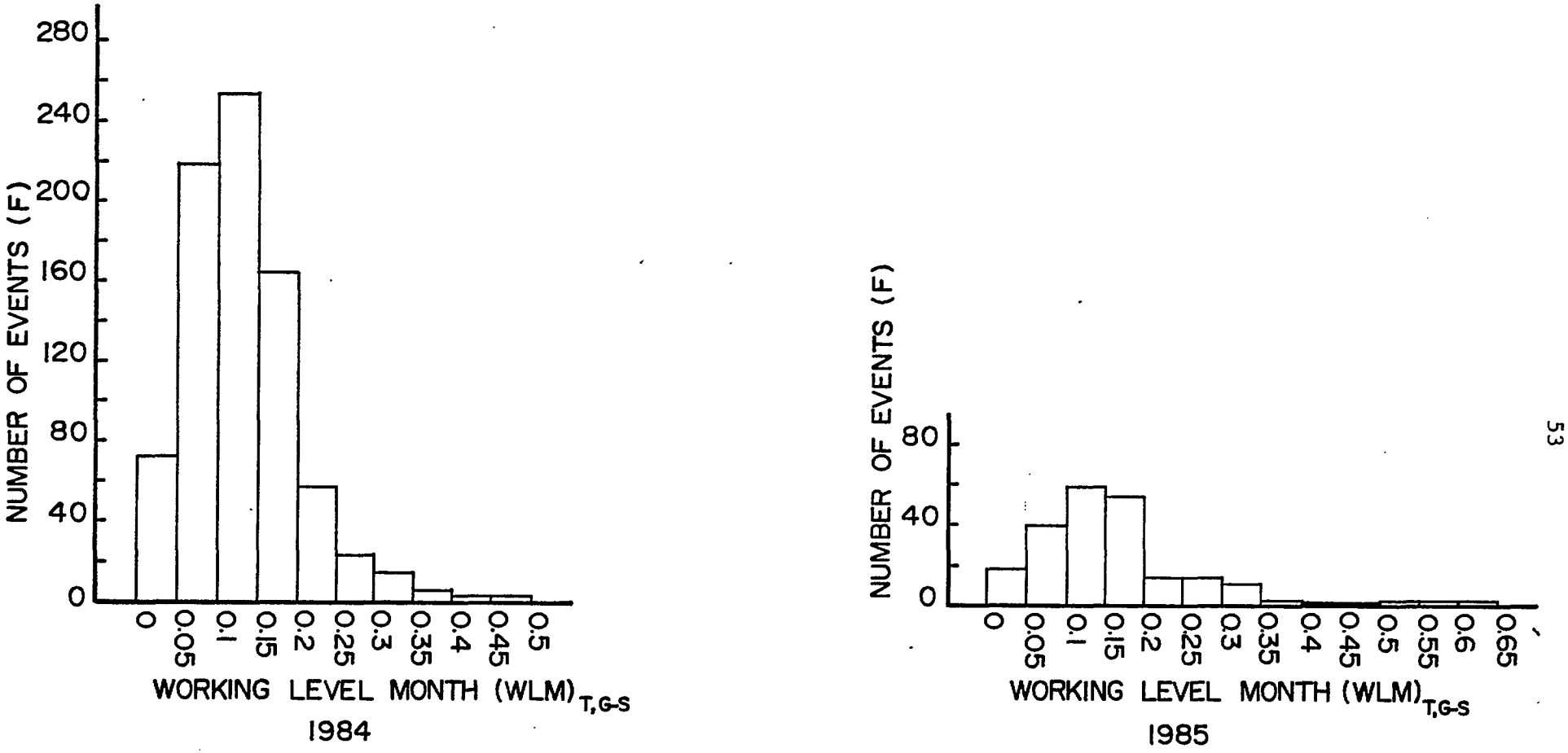

Fig. 17 - Working Level Month frequency distribution.

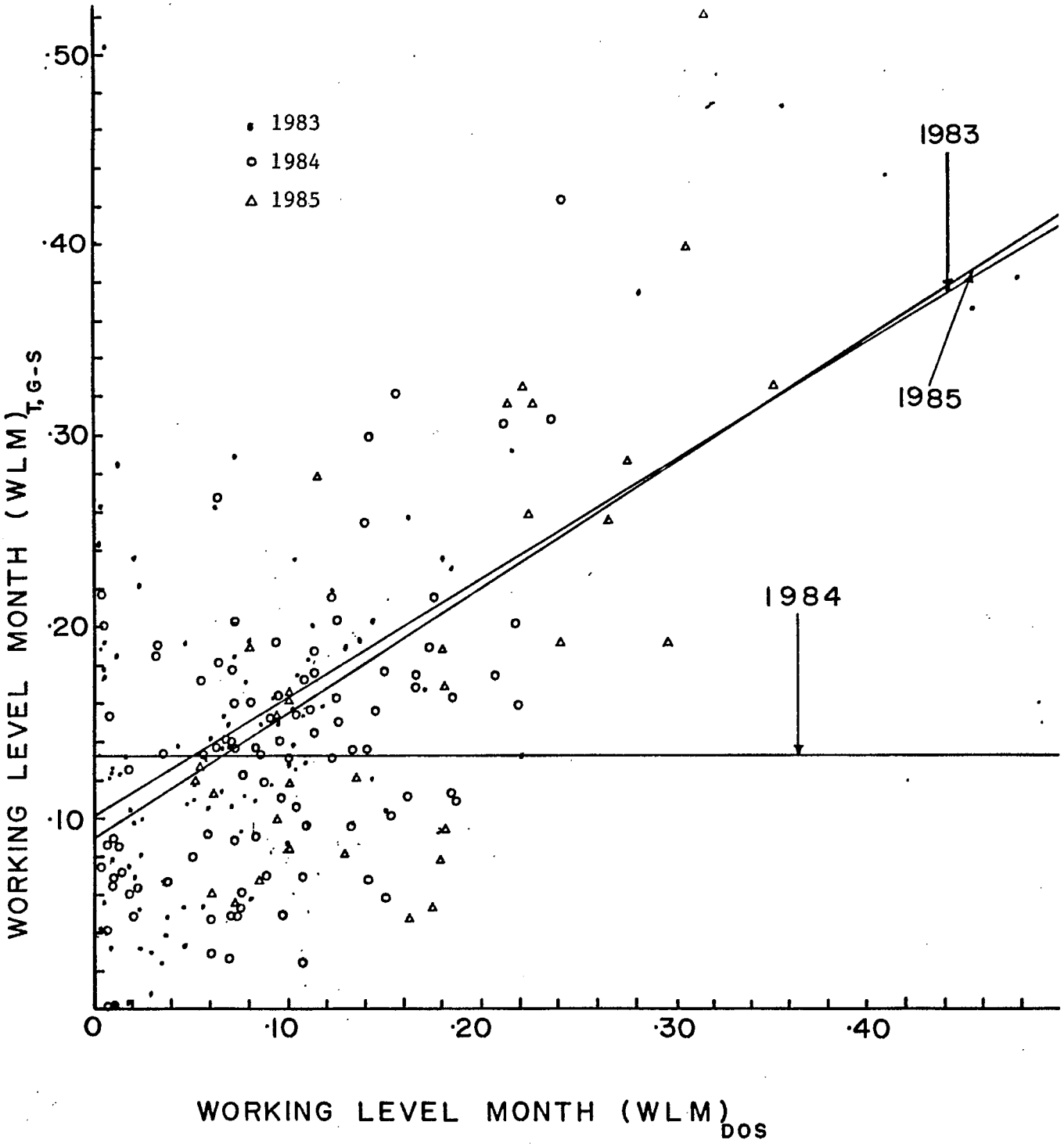

Fig. 18 - Grab-sampling Working Level Month versus dosimeter Working Level Month for a driller.

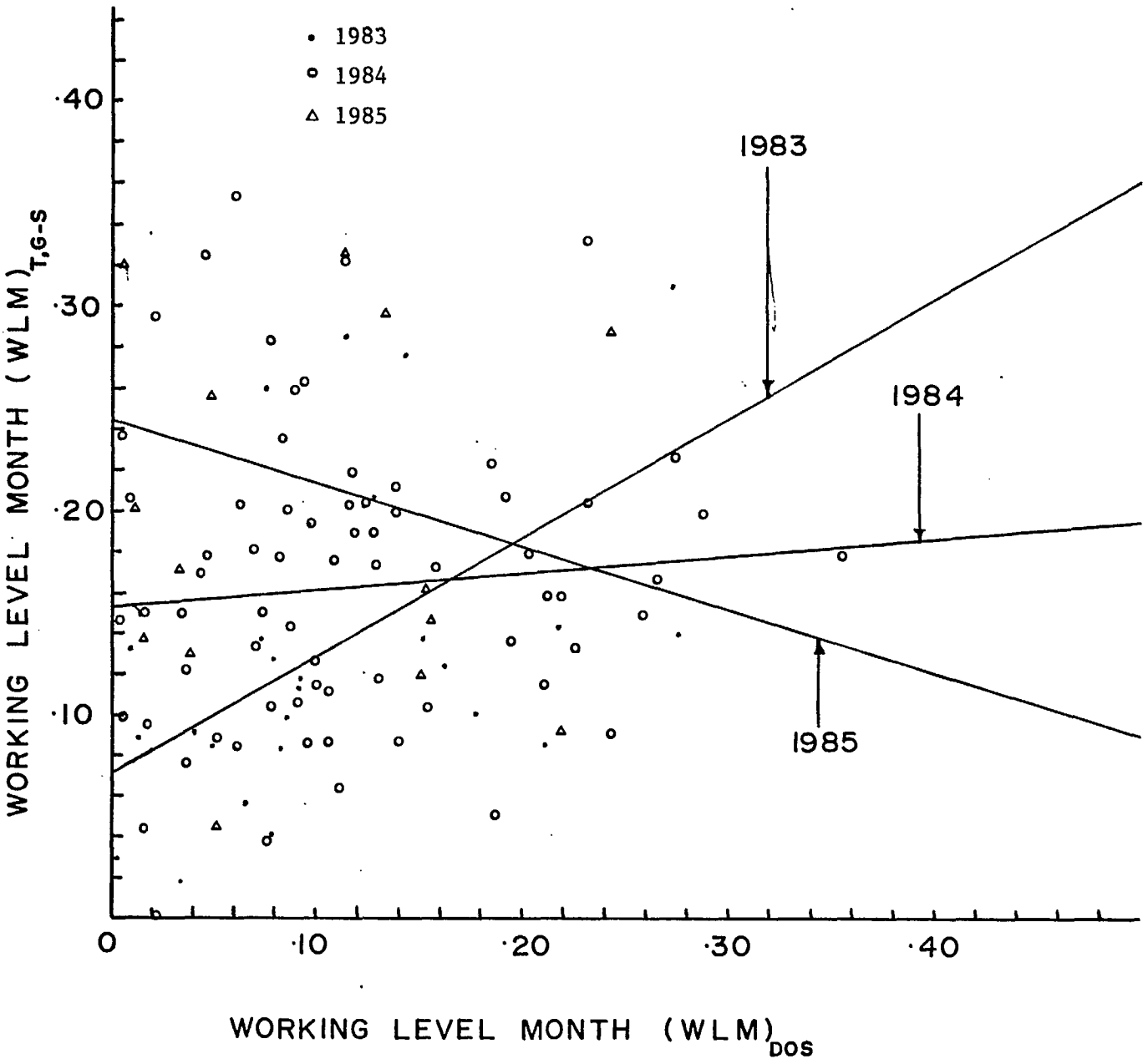

Fig. 19 - Grab-sampling Working Level Month versus dosimeter Working Level Month for a slusherman.

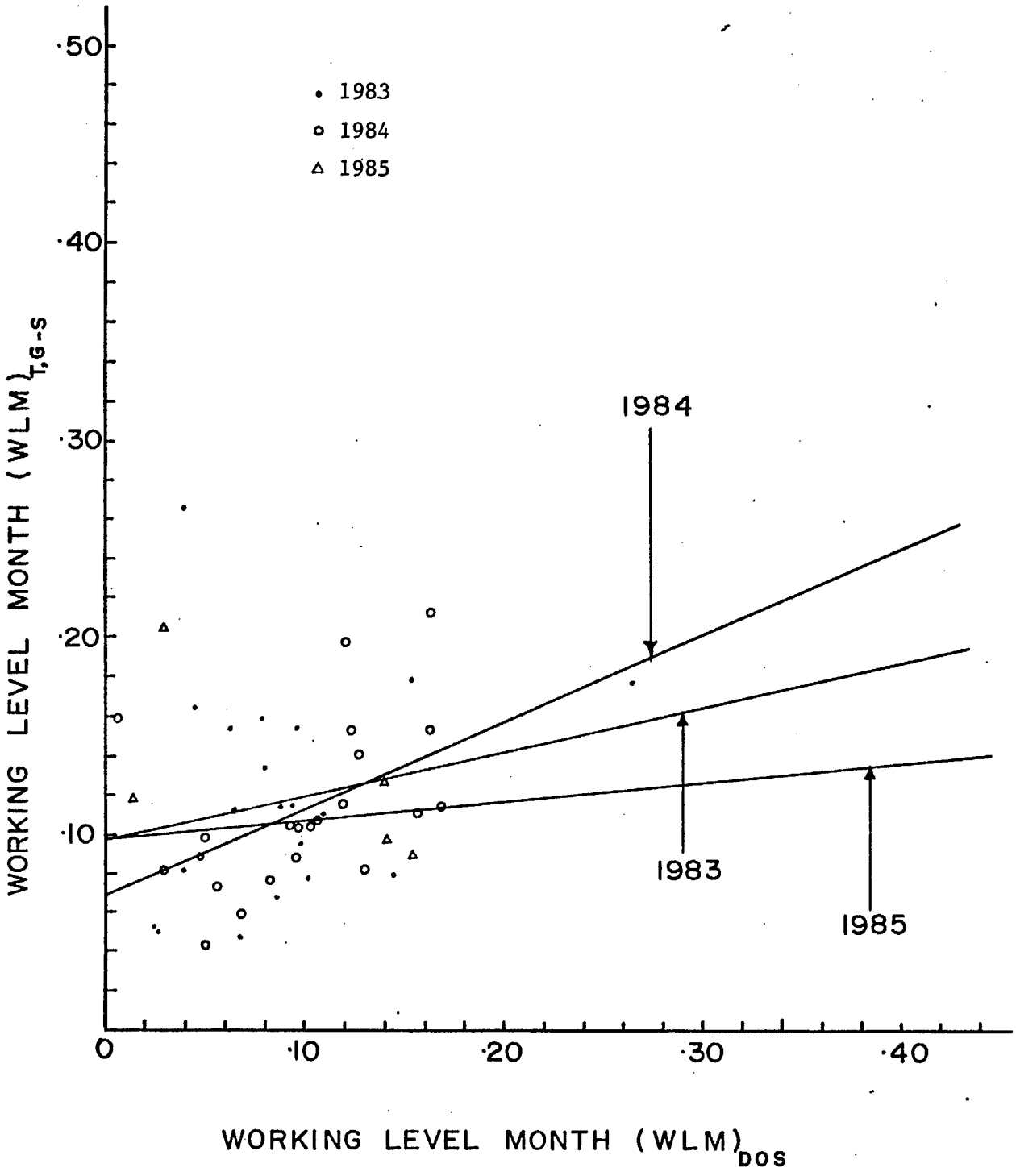

Fig. 20 - Grab-sampling Working Level Month versus dosimeter Working Level Month for a diamond driller.

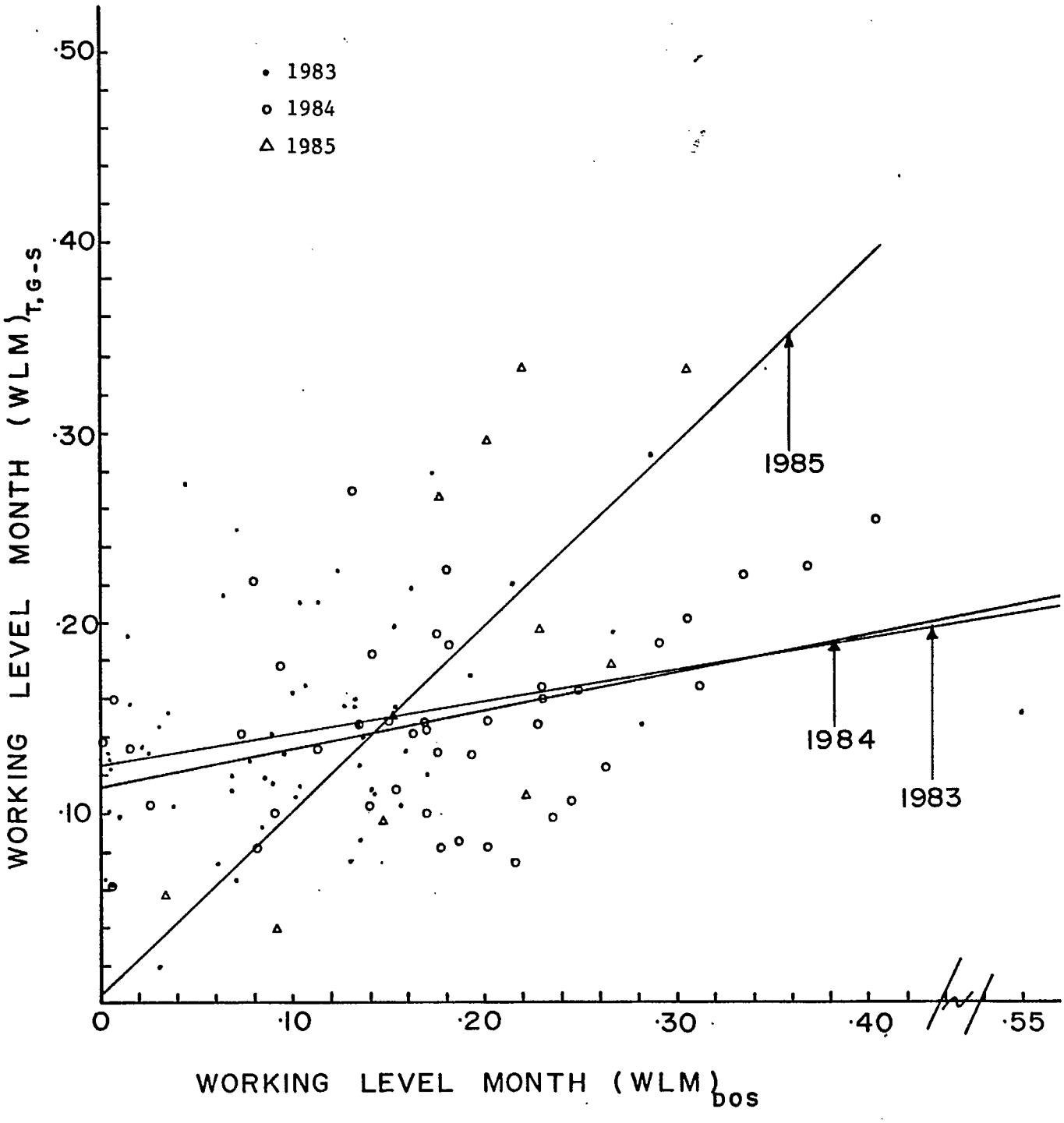

Fig. 21 - Grab-sampling Working Level Month versus dosimeter Working Level Month for a timberman.

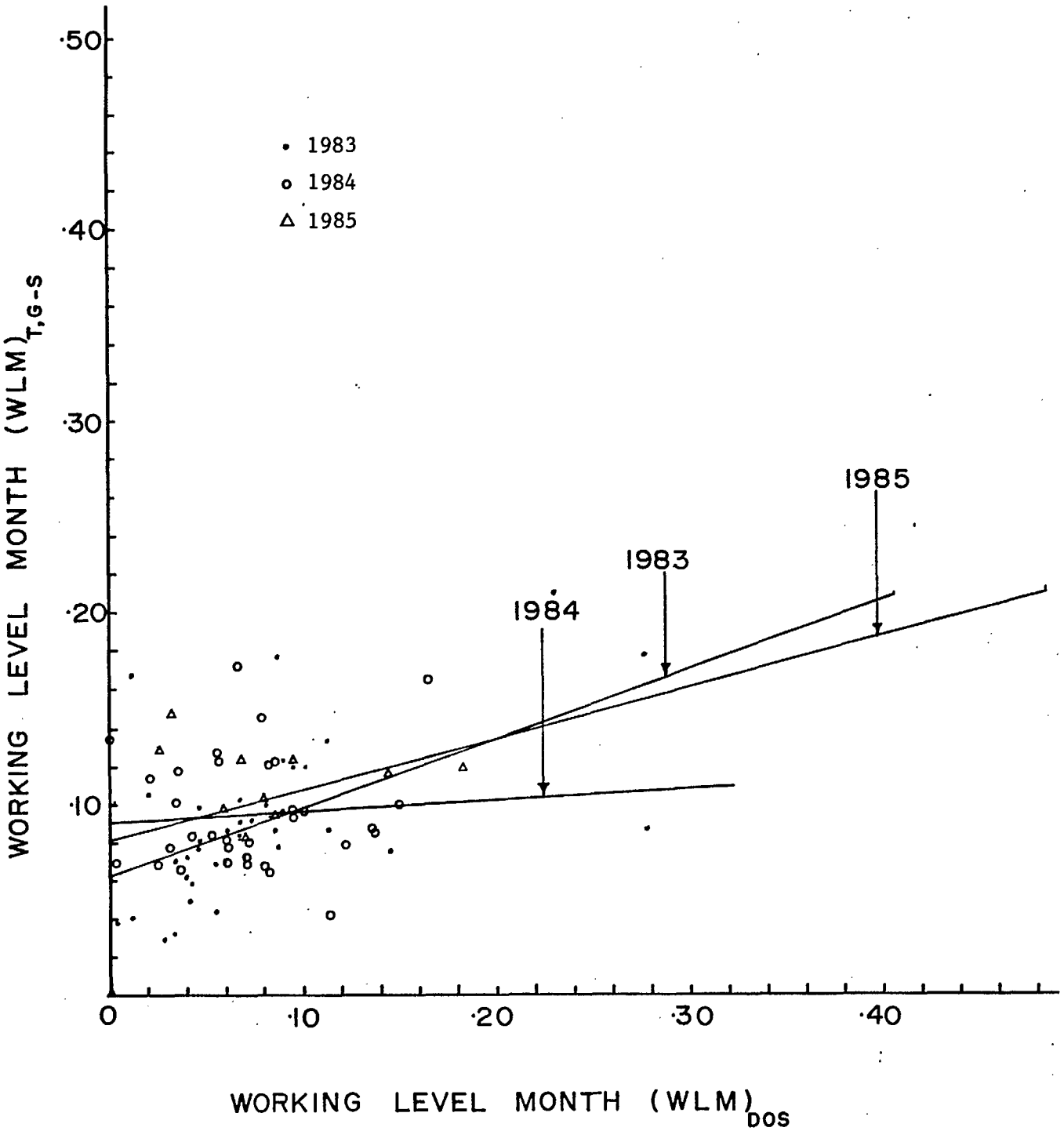

Fig. 22 - Grab-sampling Working Level Month versus dosimeter Working Level Month for a level serviceman (track).

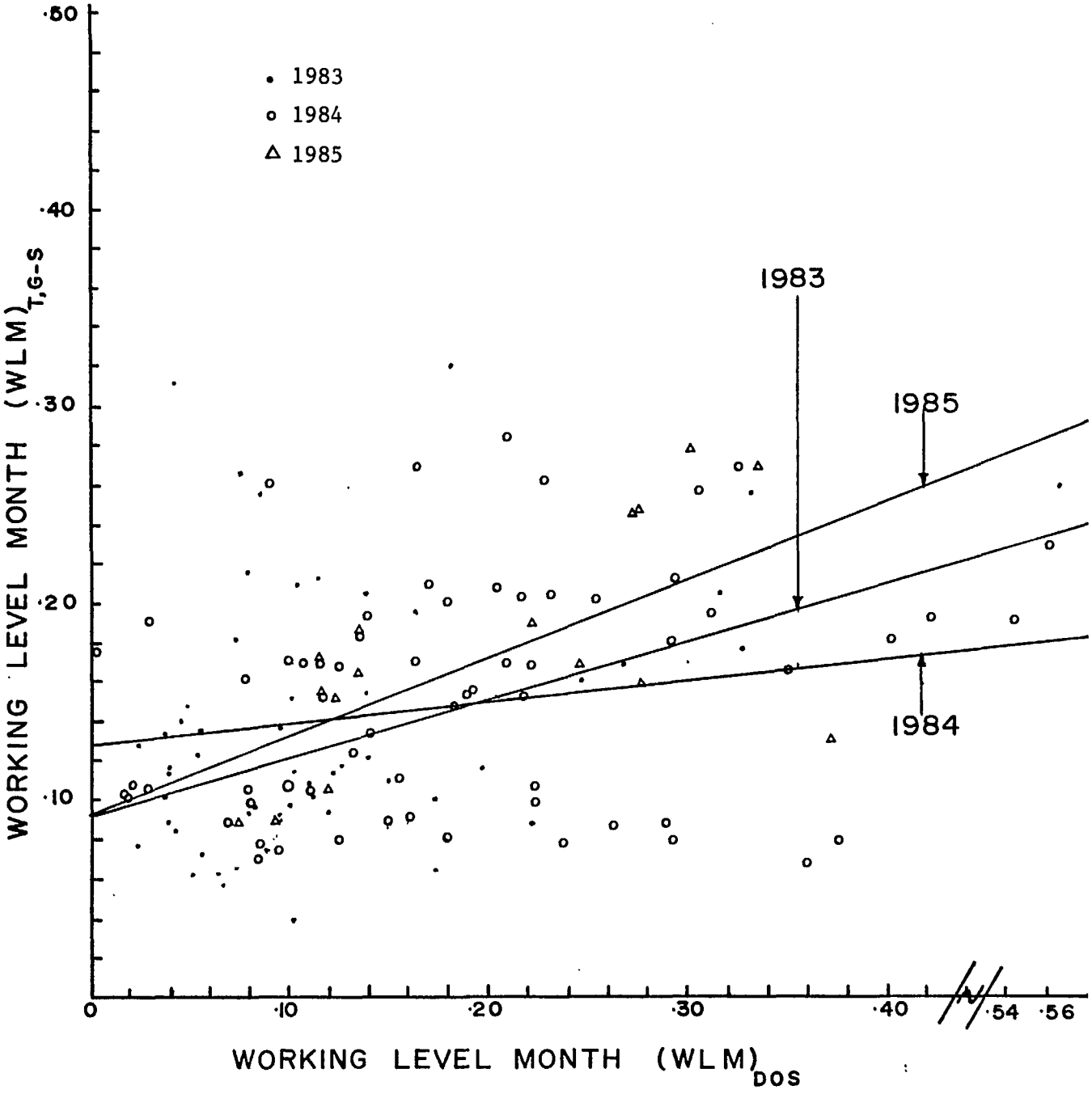

Fig. 23 - Grab-sampling Working Level Month versus dosimeter Working Level Month for a mine shift boss.

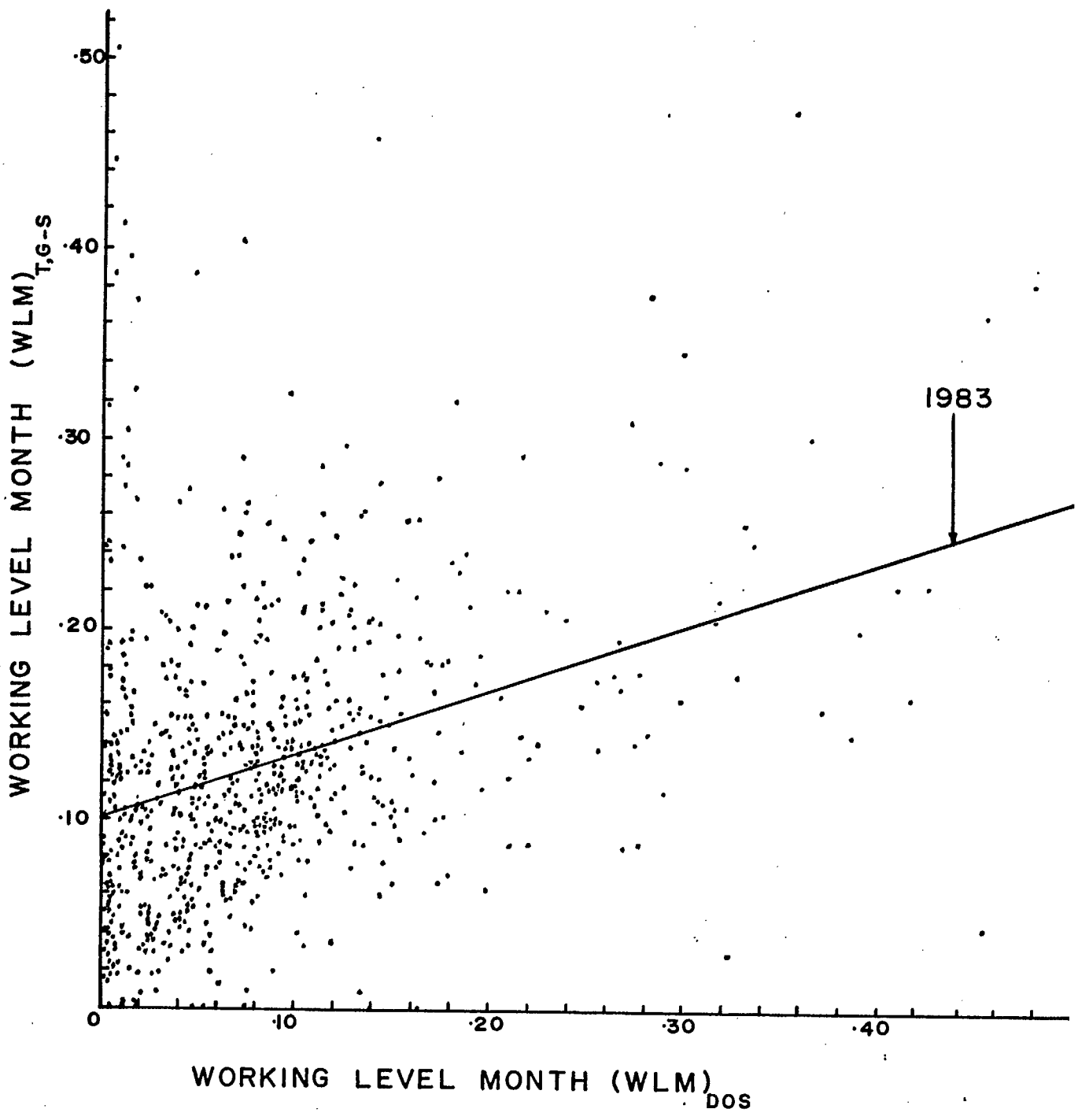

Fig. 24 - Grab-sampling Working Level Month versus dosimeter Working Level Month for 1983. Also shown is the best fitted straight line by linear regression analysis.

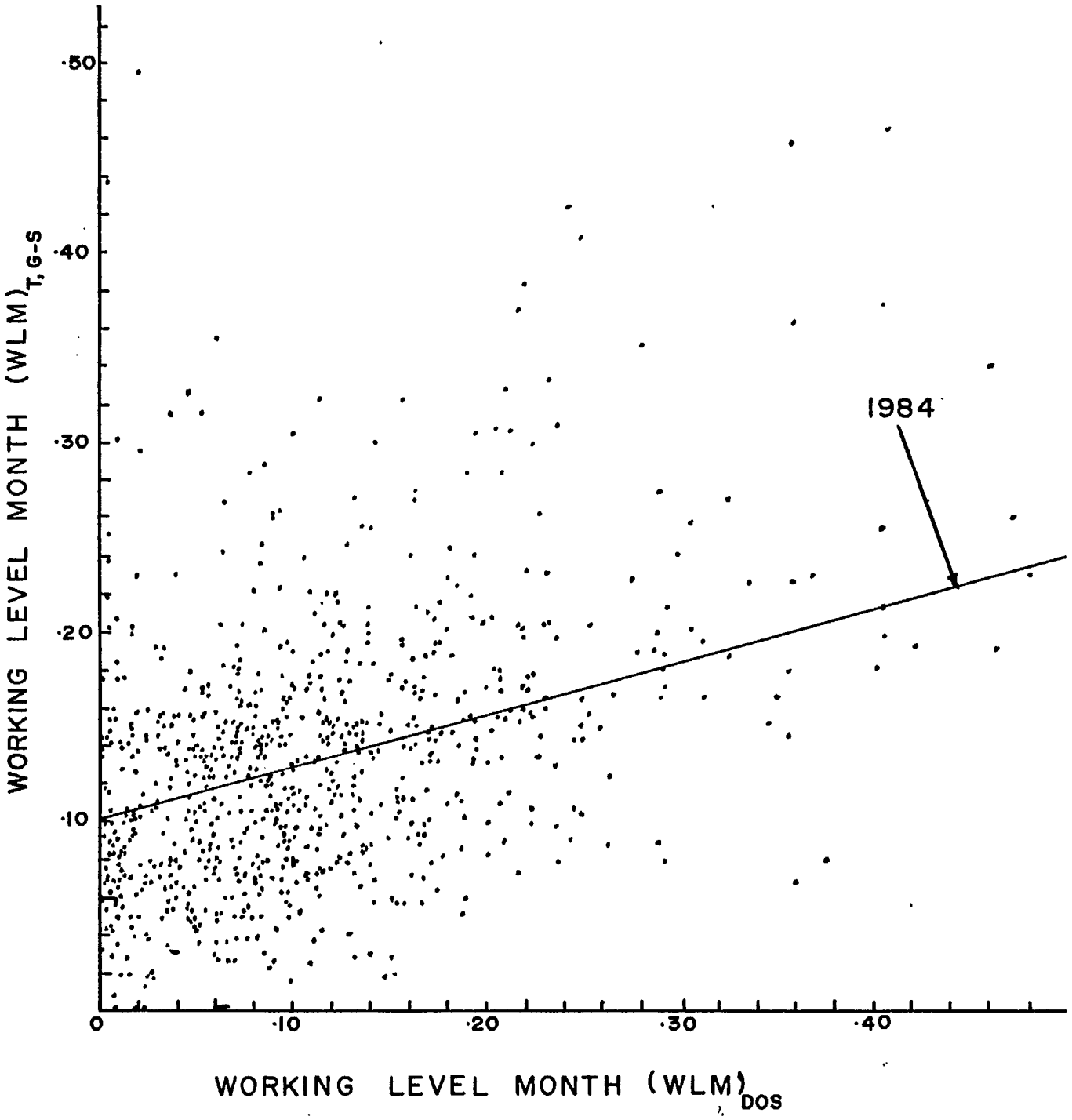

Fig. 25 - Grab-sampling Working Level Month versus dosimeter Working Level Month for 1984. Also shown is the best fitted straight line by linear regression analysis.

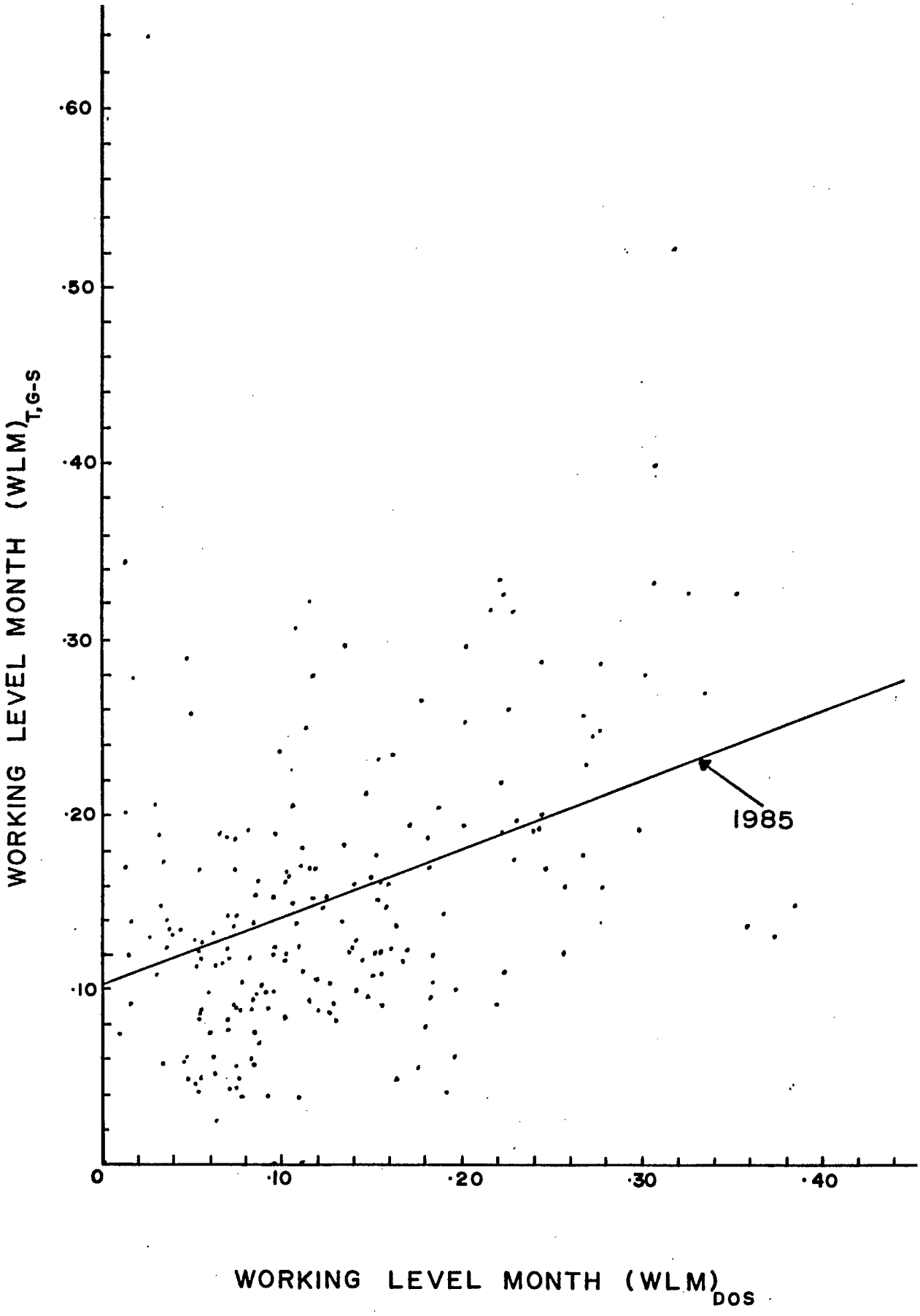

Fig. 26 - Grab-sampling Working Level Month versus dosimeter Working Level Month for 1985. Also shown is the best fitted straight line by linear regression analysis.

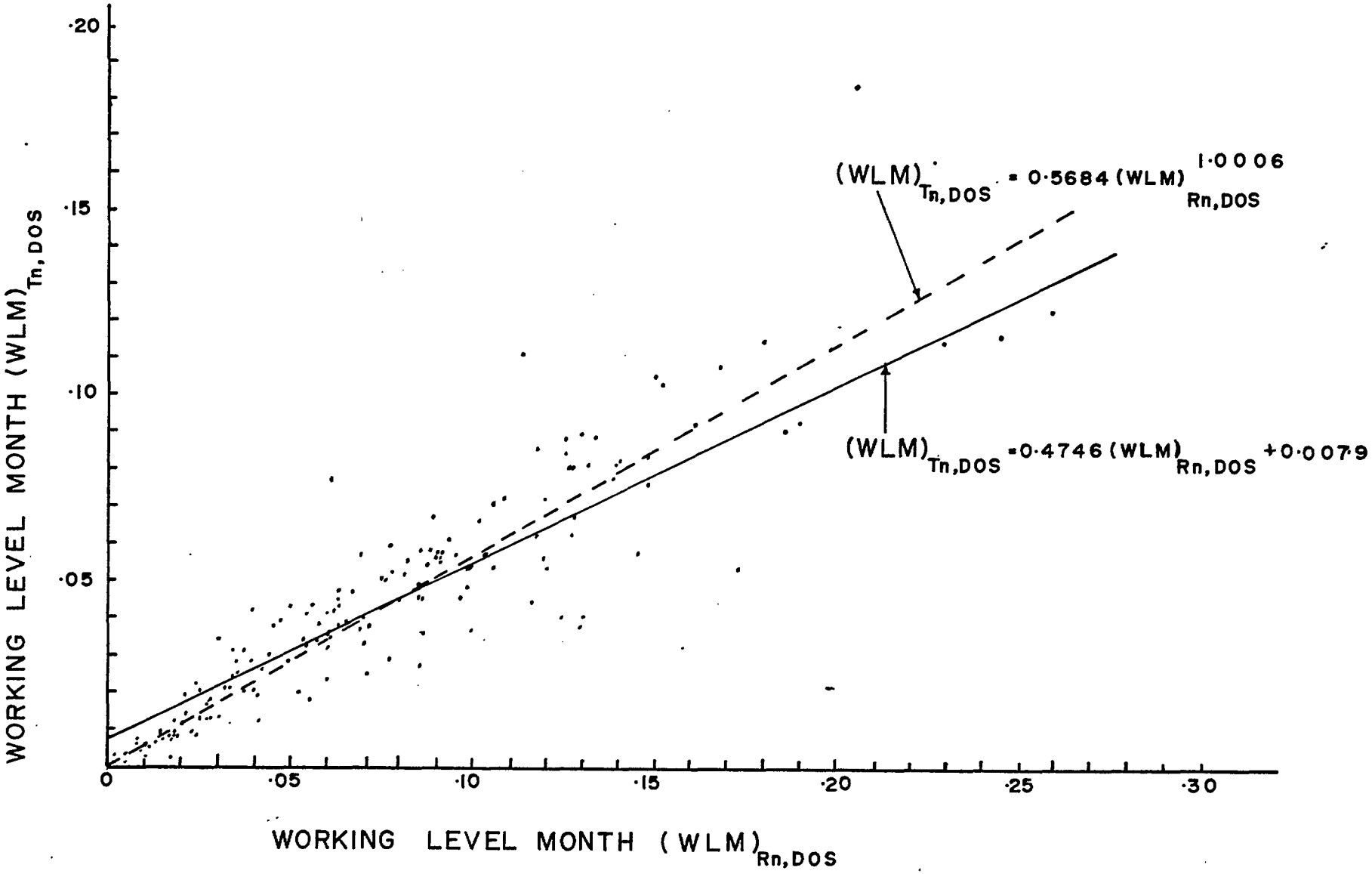

Fig. 27 - Thoron daughter Working Level Month versus radon daughter Working Level Month. Also shown are the best fitted linear and power lines by regression analysis.

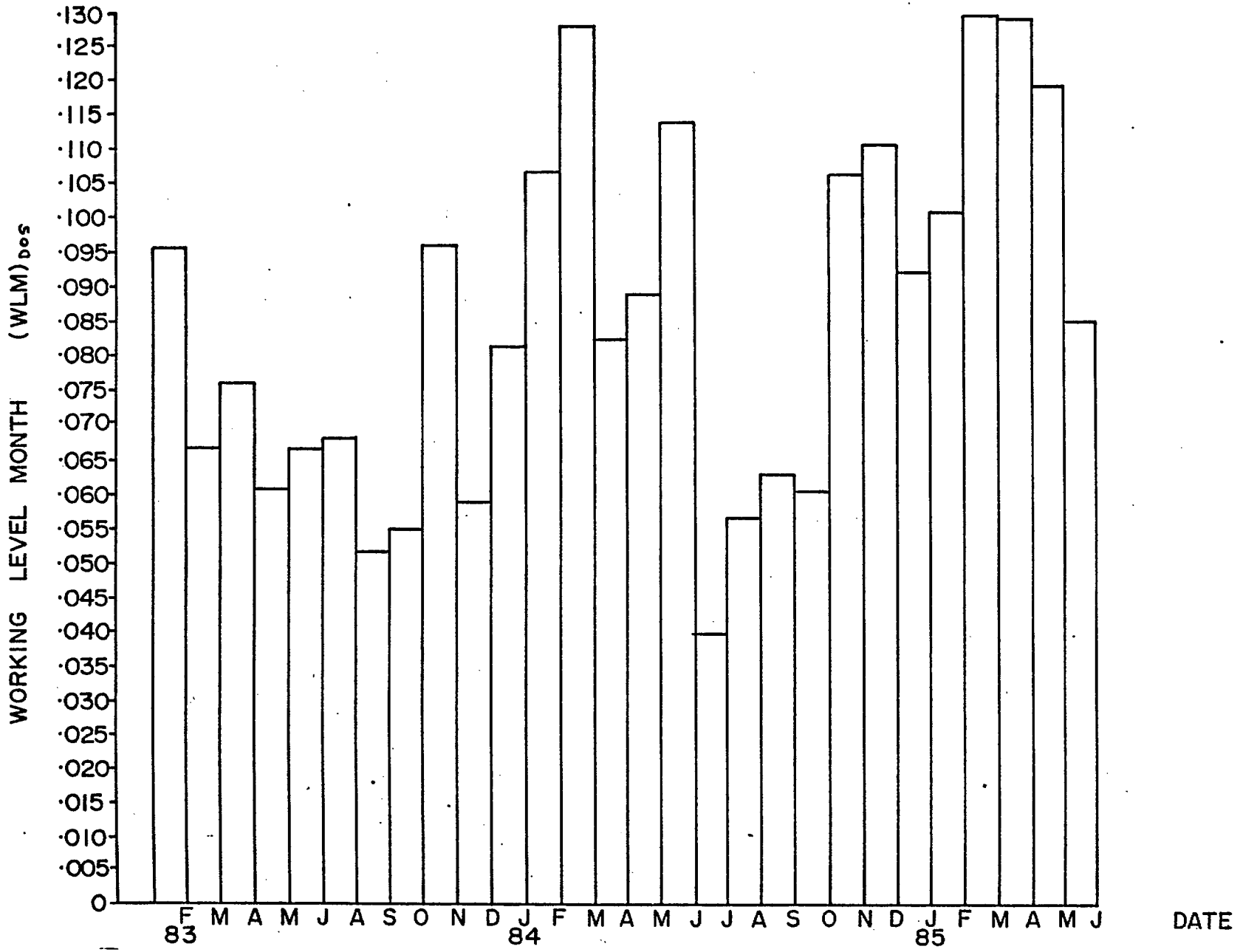

Fig. 28 - Dosimeter Working Level Month (average of all dosimeters) versus time.

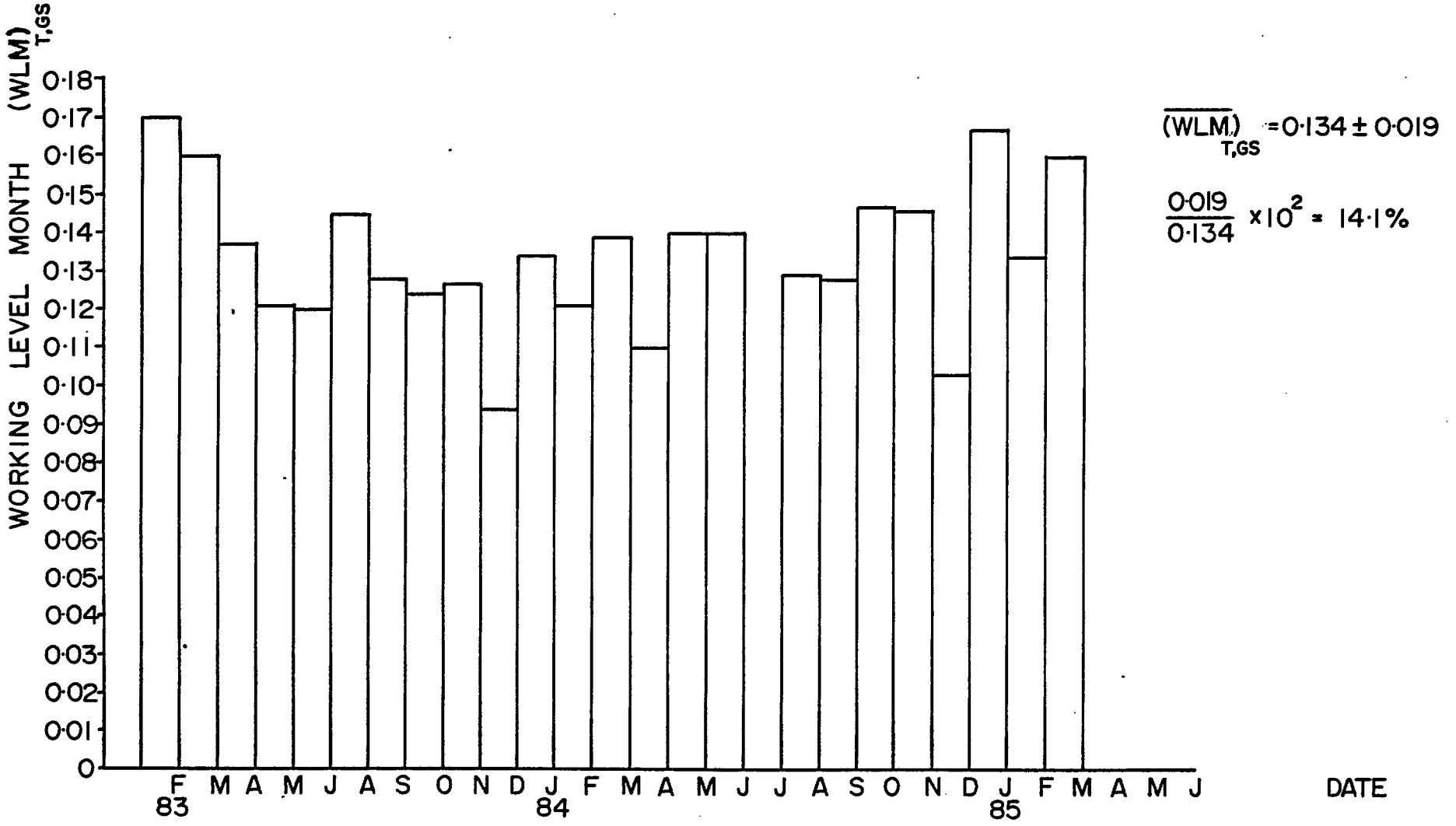

Fig. 29 - Grab-sampling Working Level Month (average of all measurements) versus time.

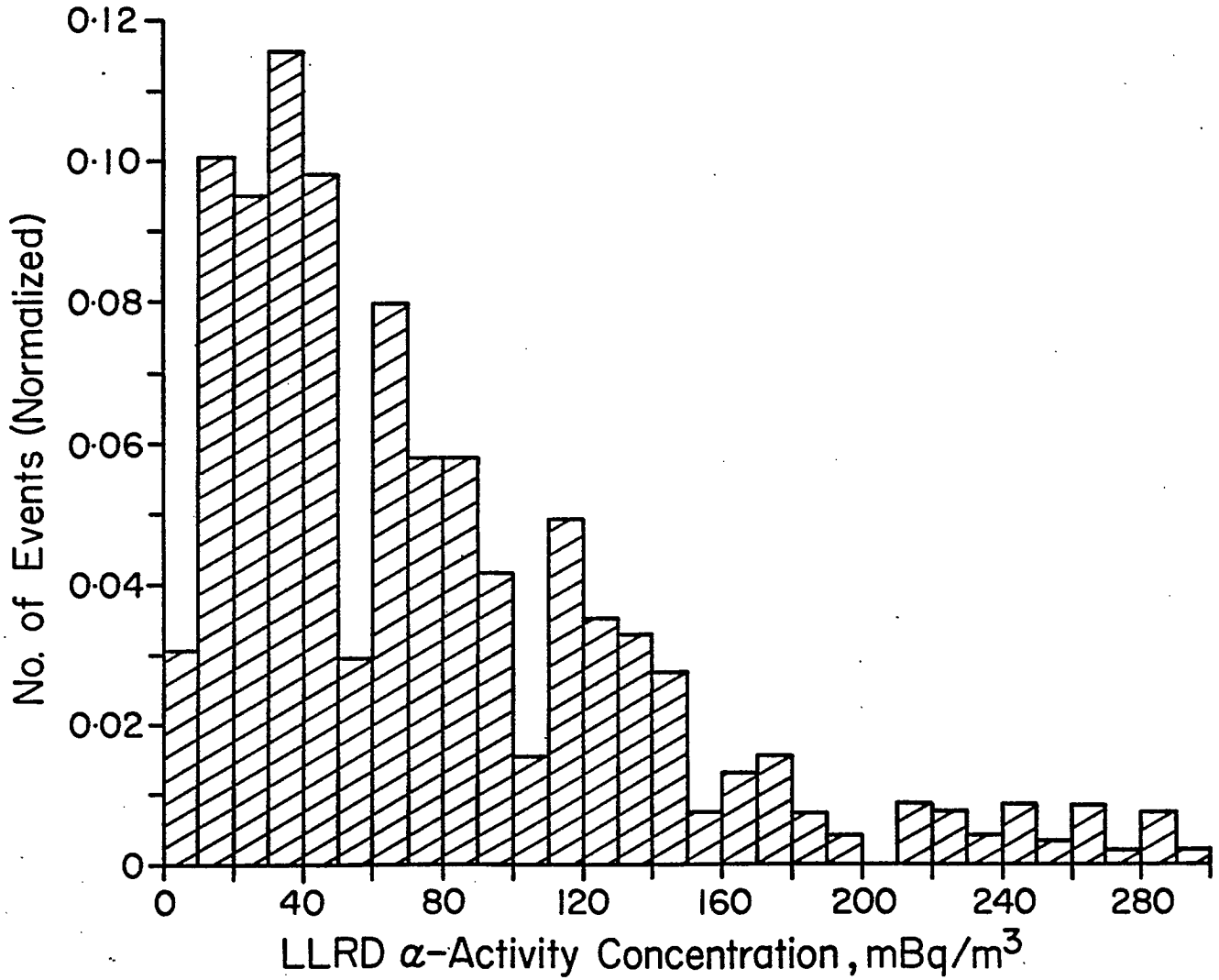

Fig. 30 - Long-Lived Radioactive Dust (LLRD) activity (concentration) distribution.

Table A.1 - Occupational codes and occupations involved in the α-particle dosimetry program (1983/85).

Occup. Code	Occupation Title
207	Mine Helper
208	Sanitation Man
209	Deckman
210	Skiptender
211	Level Service (Track)
213	Trackman
214	Pipeman Track
215	Cagetender
216	Level Service Trackless
217	Pipeman Trackless
218	U/G Mason and Gunniter
219	Bulldozer Operator
220	Timberman
221	Haulageman
227	Diamond Driller
228	Slusherman
230	Driller
231	Jumbo Drill Operator
232	L.H.D. Operator Scooptram
233	Mobile Rockbolt Machine Operator
234	Mobile Explosives Operator
236	Track Miner "A" Stope/Raise
237	Shaftman
238	Track Miner "A" Development
240	Trackless Miner "A"
242	Rockbolt Inspector
244	L.H.D.D. Operator
401	Electrical Leader
402	Electrical Journeyman
435	Industrial Mechanic Leader
436	Industrial Mechanic Journeyman
452	Welder Leader
453	Welder Journeyman
505	Drill Doctor Journeyman
540	Mobile Mechanic Leader
541	Mobile Mechanic Journeyman
553	Mobile Mechanic Apprentice #5
555	Mobile Mechanic Apprentice #7
574	Underground Crusherman
591	Environmental Inspector
592	Health and Safety Inspector
651	Survey Party Leader
652	Survey Instrument Man
679	Warehouse Clerk I
967	Underground Electrical Foreman
970	Underground Mechanical Foreman
992	Geologist
994	Mine Shiftboss

Table A.2 - Linear regression analysis data pertaining to all occupational codes during 1983, 1984 and 1985.

Occup. Code	Year	No. of Measurements	Slope (m)	Intercept (b)	Correlation Coeff., σ
207	1983	3	0.8267	0.1263	0.5796
207	1984	16	0.4815	0.0589	0.4340
207	1985	2	0.6100	0.0394	1.0000
208	1983	10	-0.0541	0.1967	-0.0909
208	1984	2	4.9833	-0.3543	1.0000
208	1985	3	-0.2322	0.2023	-0.1662
209	1983	12	-0.3306	0.1266	-0.0532
209	1984	13	-0.2550	0.0975	-0.2693
210	1983	11	-0.0123	0.0429	-0.0604
210	1984	11	0.5852	-0.0111	0.6032
210	1985	3	-0.3664	0.1103	-0.7225
211	1983	35	0.3573	0.0634	0.5544
211	1984	32	0.0557	0.0915	0.0694
211	1985	10	0.2769	0.0822	0.3712
213	1983	19	0.2583	0.1187	0.5894
213	1984	23	0.4299	0.0982	0.5331
213	1985	9	0.6864	0.0827	0.2728
214	1983	8	0.3098	0.1530	0.7857
214	1984	11	0.0375	0.1796	0.0713
214	1985	3	1.5306	-0.1733	0.9939
215	1983	10	1.7786	0.0782	0.7295
215	1984	2	-5.8235	0.3459	-1.0000
216	1983	8	-0.1592	0.1077	-0.1295
216	1984	1			
216	1985	3	-0.1065	0.2565	-0.1933
217	1983	10	1.1910	0.0279	0.6433
217	1984	7	0.4174	0.1019	0.7231
218	1983	20	0.1514	0.1442	0.1739
218	1984	11	-0.3558	0.2263	-0.4170
218	1985	3	-0.2373	0.2168	-0.4497
219	1983	7	0.3444	0.0974	0.5957
219	1984	9	-0.1645	0.2190	-0.1785
220	1983	28	0.1659	0.1261	0.2924
220	1984	44	0.2004	0.1127	0.3799
220	1985	11	0.9795	0.0042	0.7106
221	1983	32	0.1846	0.0901	0.2767
221	1984	53	0.2003	0.0991	0.1882
221	1985	9	-0.3466	0.1728	-0.2786
227	1983	20	0.2301	0.0993	0.2258
227	1984	22	0.4303	0.0699	0.4645
227	1985	5	0.0928	0.1003	0.0982

Table A.2 - Continued

Occup. Code	Year	No. of Measurements	Slope (m)	Intercept (b)	Correlation Coeff., σ
228	1983	25	0.5801	0.0730	0.7186
228	1984	69	0.0835	0.1529	0.0940
228	1985	15	-0.3126	0.2453	-0.1914
230	1983	92	0.6169	0.1024	0.5645
230	1984	97	0.0017	0.1327	0.0495
230	1985	33	0.6492	0.0912	0.4172
231	1983	1			
231	1984	21	0.0409	0.1377	0.1153
231	1985	6	-0.2293	0.2043	-0.4156
232	1983	0			
232	1984	11	0.0483	0.1313	0.1034
232	1985	5	0.7736	0.0177	0.8596
233	1984	9	0.0077	0.3156	0.1130
234	1984	6	-0.2994	0.1129	-0.7364
234	1985	3	-0.9223	0.1403	-1.0000
236	1983	25	0.3757	0.0851	0.2047
236	1984	41	0.0082	0.0918	0.0116
236	1985	4	0.1365	0.0889	0.4629
237	1983	10	0.3282	0.0769	0.5305
237	1984	11	0.3853	0.0630	0.4396
237	1985	3	-1.7171	0.3006	-0.9998
238	1984	11	0.0205	0.0878	0.0339
238	1985	3	1.7009	-0.0103	0.9977
240	1983	29	0.0380	0.1662	0.0110
240	1984	22	0.8692	0.0879	0.6531
240	1985	3	-0.2815	0.1879	-0.3584
242	1984	1			
244	1983	10	-1.3207	0.3306	-0.5360
244	1984	14	0.0496	0.2845	0.0556
244	1985	3	2.9135	0.0423	0.4702
401	1983	1			
402	1983	10	0.4859	0.0937	0.3435
402	1984	18	0.0110	0.1281	0.0364
402	1985	3	-0.3016	0.1440	-0.5105
435	1983	8	3.4134	0.0740	0.8277
436	1983	10	0.3936	0.1145	0.6239
436	1984	2	-0.4290	0.1328	-1.0000
436	1985	3	-0.0158	0.1536	-0.1705
452	1983	9	-0.8791	0.0286	-0.2138
453	1984	4	-1.5141	0.1977	-0.8694
505	1983	11	0.0384	0.1368	0.1088
505	1985	3	-0.0316	0.1480	-0.0216

Table A.2 - Continued

Occup. Code	Year	No. of Measurements	Slope (m)	Intercept (b)	Correlation Coeff., σ
540	1983	1			
540	1984	12	1.2337	0.0438	0.8063
541	1983	37	0.1478	0.1324	0.2882
541	1984	36	0.3336	0.1072	0.2952
541	1985	10	0.0338	0.1436	0.0516
553	1983	10	-0.0254	0.1242	-0.0398
555	1984	11	0.9778	0.0171	0.8088
555	1985	3	0.4004	0.1042	0.4568
574	1983	20	-0.0714	0.1518	-0.0662
574	1984	17	0.5405	0.0782	0.4822
574	1985	6	0.1612	0.1265	0.6439
591	1983	15	0.3022	0.0571	0.2656
591	1984	11	0.1944	0.0441	0.6150
591	1985	3	-0.2460	0.0593	-0.9614
592	1983	10	-0.3655	0.0655	-0.2982
592	1984	11	0.0145	0.0413	0.2268
592	1985	3	-0.7583	0.0964	-0.9847
651	1983	1			
651	1984	3	-0.4716	0.0689	-0.9939
651	1985	3	0.8251	-0.0144	0.6875
652	1983	1			
652	1985	3	4.0977	-0.4008	0.5636
679	1983	5	0.5704	-0.0061	0.9606
967	1983	20	0.0954	0.0851	0.1211
967	1984	22	0.2851	0.0707	0.3424
967	1985	5	-0.8360	0.2321	-0.6054
970	1983	20	0.4132	0.0671	0.6761
970	1984	11	0.2502	0.1258	0.4010
970	1985	3	-1.7057	0.3507	-0.8610
992	1983	11	0.4028	0.0235	0.4478
992	1984	8	0.0607	0.0354	0.0391
992	1985	2	-0.0147	0.0485	-1.0000
994	1983	58	0.2960	0.0930	0.4360
994	1984	65	0.1105	0.1273	0.2157
994	1985	15	0.4009	0.0931	0.6406

Note: Data fitted to a straight line of the form:

$$(WLM)_{T,GS} = m(WLM)_{DOS} + b$$